EFFECT OF SIZE, TEMPERATURE AND STRAIN RATE ON DEFORMATION BEHAVIOUR OF NICKEL NANOWIRES: A MOLECULAR DYNAMICS SIMULATION STUDY

A Thesis submitted in partial fulfillment of the requirements for the Degree

Of

Bachelor in Technology (B. Tech)

In

METALLURGICAL & MATERIALS ENGINEERING

By

GAURAV MEHTA (109MM0448)

HRUSHIKESH PATRA (109MM0452)

Department of Metallurgical & Materials Engineering
National Institute of Technology
Rourkela-769008
2013

EFFECT OF SIZE, TEMPERATURE AND STRAIN RATE ON DEFORMATION BEHAVIOUR OF NICKEL NANOWIRES: A MOLECULAR DYNAMICS SIMULATION STUDY

A Thesis submitted in partial fulfillment of the requirements for the Degree

Of

Bachelor in Technology (B. Tech)

In

METALLURGICAL & MATERIALS ENGINEERING

By

GAURAV MEHTA (109MM0448)

HRUSHIKESH PATRA (109MM0452)

Under the Guidance of

Prof. N. YEDLA

Department of Metallurgical & Materials Engineering
National Institute of Technology
Rourkela-769008
2013

DEPARTMENT OF METALLURGICAL & MATERIALS ENGINEERING

NATIONAL INSTITUTE OF TECHNOLOGY

ROURKELA-769008, INDIA

CERTIFICATE:

This is to certify that the project entitled "**Effect of size, temperature and strain rate on deformation behaviour of nickel nanowires: A molecular dynamics simulation study**" submitted by **Mr. GAURAV MEHATA (109MM0448) and Mr. HRUSHIKESH PATRA (109MM0452)** in partial fulfillments for the requirements for the award of **Bachelor of Technology** Degree in **Metallurgical & Materials Engineering** at **National Institute of Technology, Rourkela** (Deemed University) is an authentic work carried out by them under my supervision and guidance.

To the best of my knowledge, the matter embodied in the report has not been submitted to any other University / Institute for the award of any Degree or Diploma.

DATE: 08.05.2013

Prof. N. YEDLA

Department of Metallurgical & Materials Engineering

National Institute of Technology

Rourkela-769008

ACKNOWLEDGEMENT

We would like to thank **NIT Rourkela** for giving us the opportunity to use its resources and work in such a challenging environment. First and foremost, we take this opportunity to express our deep regards and sincere gratitude to our guide **Prof. N. Yedla** for his able guidance and constant encouragement during our project work. This project would not have been possible without his help and the valuable time that he has given us amidst his busy schedule.

We would also like to express our utmost gratitude to **Prof. B.C Ray, HOD, Metallurgical & Materials engineering** for allowing us to use the departmental facilities and for his valuable suggestions and encouragements at various stages of the work.

We would also like to extend our hearty gratitude to our friends and senior students of this department who have always encouraged and supported in doing our work. Last but not the least, we would like to thank all the staff members of Department of Metallurgical &Materials Engineering who have been very cooperative with us.

Place: NIT Rourkela **Gaurav Mehta (109MM0448)**

Date: 08.05.2013 **Hrushikesh Patra (109MM0452)**

Department of Metallurgical & Materials Engineering

National Institute of Technology

Rourkela-769008

ABSTRACT

Metallic Nanowires have attracted considerable attention due to their unique properties and have been evolved as a potential field of research in recent years. The recent discovery of new metallic nanomaterials makes it possible to produce nanometarials in bulk shapes. Bulk metallic nanowires provide a promising future to revolutionize the field of structural materials with combinations of strength, elastic limit, toughness, wear resistance and corrosion resistance.

Since the fabrication and deformation studies of metallic nanowires are sometimes practically impossible in laboratory conditions, so computational approaches are extensively used to explore various properties and behaviour of metallic nanowires.

This project work presents a molecular dynamics simulation study on deformation behaviour of Nickel nanowire where the effect of parameters like sample-size, strain rate and temperature on the tensile deformation behaviour have been thoroughly studied. Computational methods to create metallic nanowire models and further tensile deformation have been mentioned. Stress-strain plots were drawn at same strain rate for different sizes of nanowire models, at different temperatures for particular strain rate and size and at different strain rates for a particular size and temperature. Reasons for getting different stress-stress curves and mechanical properties for different conditions have also been discussed.

CONTENTS

List of Figures:

List of tables:

Chapter-1

Introduction

1.1 Introduction to Nanowires:

Development and improvement in technology of engineering devices depends on availability of innovative materials which are capable of withstanding the most stringent service conditions. The need of innovative materials make the way for scientists to find out new materials for most stringent service conditions. Materials with nano level microstructural features make up such class of materials that has caught the imagination of researchers worldwide. Nanomaterials have their potential to exhibit very unusual combinations of properties. Here the focus of this project work on the nanowires.

A nanowire is a nanostructure with the diameter of the order of a nanometer (10^{-9} meters). Nanowires can be defined as the structures that have a thickness or diameter constrained to tens of nanometers or less and an unconstrained length.

At these scales, quantum mechanical effects are important which coined the term "quantum wires". Many different types of nanowires exist, including metallic, semiconducting and insulating. Metallic nanowires are like Ni, Pt and Au nanowires. Semiconducting nanowires are like Si, InP & GaN. Insulating nanowires are like SiO_2 & TiO_2 [1].

Typical nanowires exhibit aspect ratios (length-to-width ratio) of 1000 or more. As such they are often referred to as one-dimensional (1-D) materials. Nanowires have many interesting properties that are not seen in bulk or 3-D materials. This is because electrons in nanowires are quantum confined laterally and thus occupy energy levels that are different from the traditional continuum of energy levels or bands found in bulk materials.

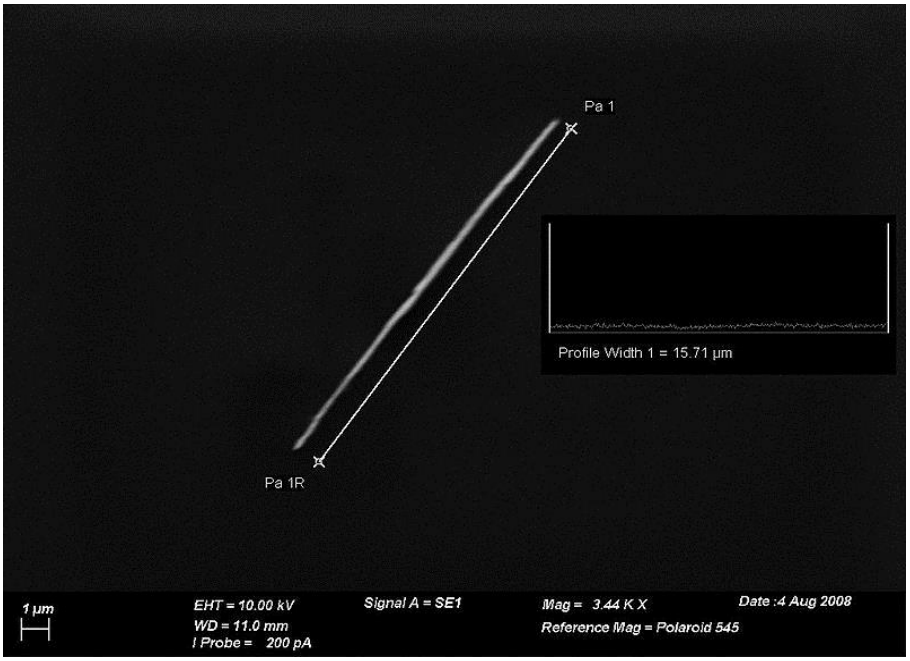

Fig. 1.1 An SEM image of a 15 micrometer Ni nanowire [1]

1.2 Nanowires: A beginning:

In last century's final decade there was a revolution in terms of new and powerful experimental techniques, such as atomic force microscopy (AFM), Scanning Tunneling Microscopy (STM) and high resolution transmission electron microscopy (HRTEM).

These new techniques revolutionized the understanding of matter at its atomic level and some of techniques allow atomic manipulation. As a consequence, nano science became a reality, and research in nanophysics is one of the important efforts nowadays [2].

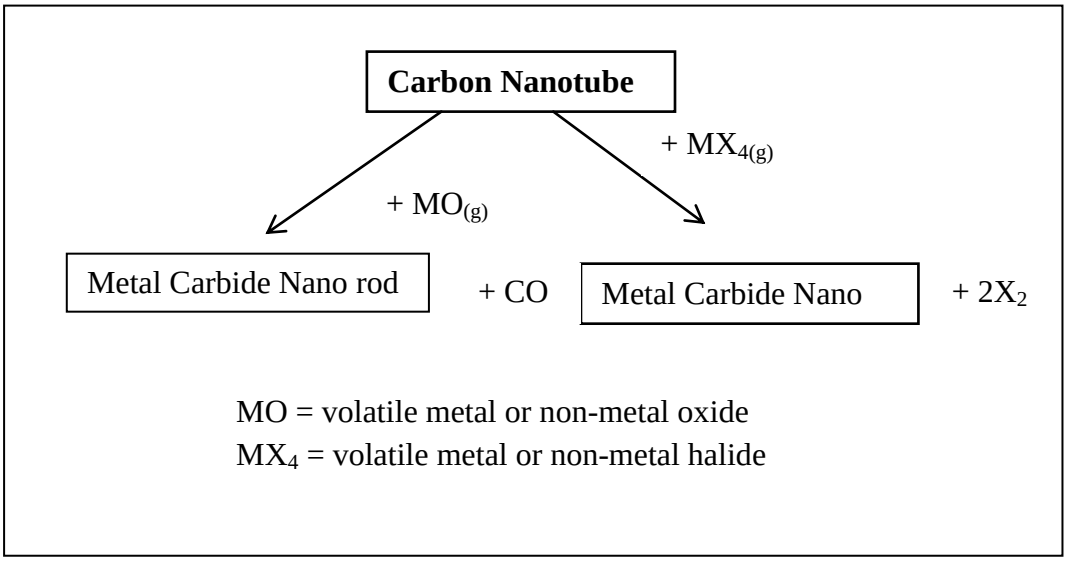

Carbide Nanowire	**Metal Reactants**	**Nanowire Structure**	**Properties**
TiC	TiO or Ti + I_2	Single Crystal	Metal
NbC	Nb + I_2	Polycrystalline	Superconductor
Fe_3C	$FeCl_3$	Amorphous	Ferromagnetic
SiC	SiO or Si + I_2	Single Crystal	Semiconductor
BC_x	B_2O_2	Polycrystalline	Insulator

Fig.1.2 Reaction scheme used to prepare metal carbide nanowire

1.3 Synthesis of Nanowires[1]:

There are 2 basic approaches to synthesize the nanowires: (i) top-down & (ii) bottom-up.

(i)Top-down: A top-down approach reduces a large piece of material to small pieces, by various means such as electrophoresis or lithography**.**

(ii)Bottom-up: A bottom-up approach synthesizes the nanowire by combining constituent atoms. Most of the synthesis techniques use a bottom-up approach.

Nanowire production uses several common laboratory techniques, including vapor deposition, electrochemical deposition, suspension & VLS (vapour-liquid-solid) growth.

- **Suspension:** A suspended nanowire is a wire produced in a high-vacuum chamber held at the longitudinal extremities. Suspended nanowires can be produced by:
  - Chemical etching of a larger wire.
  - Bombardment of a larger wire, normally with highly energetic ions.
  - Indenting the tip of a STM (Scanning Tunneling Microscope) in the surface of a metal near its melting point and then retracting it.

- **VLS growth:** Vapor-Liquid- Solid (VLS) synthesis can produce crystalline nanowires of some semiconductor materials. It uses as source material either laser ablated particles or a feed gas such as silane**.** The synthesis requires a catalyst. For nanowires, the best catalysts are liquid metal (such as gold) nanoclusters, which can either be self-assembled from a thin film by dewetting, or purchased in colloidal form and deposited on a substrate. The source enters these nanoclusters and begins to saturate them. On reaching supersaturation, the source solidifies and grows outward from the nanocluster. Simply turning off the source can adjust the final length of the nanowire. Switching sources while still in the growth phase can create compound nanowires with super-lattices of alternating materials.

- **Solution phase synthesis:** This synthesis refers to techniques the grow nanowires in solution. Solution phase synthesis can produce nanowires of many types of material. This technique can produce very large quantities compared to other method. This technique is particularly versatile at producing nanowires of and silver, lead & platinum.

The supercritical fluid-liquid-solid growth method can be used to synthesize semiconductor nanowires (for example Si and Ge). By using metal nanocrystals as seeds, Ge & Si organometallic precursors are fed into a reactor filled with a supercritical organic solvent, such as toluene. Thermolysis results in degradation of the precursor, allowing release of Si or Ge, and dissolution into the metal nanocrystals. As more of the semiconductor solute is added from the supercritical phase a solid crystallite precipitates, and a nanowire grows uniaxially from the nanocrystal seed.

1.4 Physics of Nanowires[1]:

- **Conductivity of nanowires:** The conductivity of a nanowire will be much less than that of the corresponding bulk material. Nanowires also show other peculiar electrical properties due to their size. Unlike carbon nanotubes, whose motion of electrons can fall under the regime of ballistic transport, nanowire conductivity is strongly influenced by edge effects. The edge effects come from atoms that lay at the nanowire surface and are not fully bonded to neighboring atoms like the atoms within the bulk of the nanowire. The conductivity can undergo a quantization in energy; that is the energy of the electrons going through a nanowire can assume only discrete values, which are multiples of the Von Klitzing constant $G=2e^2/h$(where 'e' is the charge of the electron and h is the Planck constant).
- **Welding nanowires:** To incorporate nanowire technology into industrial applications, researchers in 2008 developed a method of welding nanowires together; a sacrificial metal nanowire is placed adjacent to the ends of the pieces to be joined (using the manipulators of a scanning electron microscope); then an electric current is applied, which fuses the wire ends. Recently scientists discovered that single-crystalline ultrathin gold nanowires with diameters ~3-10 nm can be "cold-welded" together within seconds by mechanical contact alone, and under remarkably low applied

pressures.

High-resolution transmission electron microscopy and in situ measurements reveal that the welds are nearly perfect, with the same crystal orientation, strength and electrical conductivity as the rest of the nanowire. The high quality of the welds is attributed to the nanoscale sample dimensions, oriented-attachment mechanisms and mechanically assisted for surface diffusion

1.5 Deformation mechanism in Nanowires[2]:

The expansion of the understanding of deformation of conventional polycrystalline materials to materials with grain sizes in the range of nanometer is, at present, an evolving process. Though several mechanisms have been proposed, there still exists widespread disagreement in the research community. Most striking of all is the observation of ‘‘Inverse Hall–Petch’’ phenomenon which is still in question ever since Chokshi and others reported it in 1989.

- **Pile-up breakdown:** The concept of pile-ups has been at the root of the traditional explanation for the Hall-Patch effect. As the grain size is decreased, the number of dislocations piled up against a grain boundary decreases, at a fixed stress level, since this number is a function of the applied stress and of the distance to the source. Conversely, an increased stress level is needed to generate the same number of dislocations at the pile-up. At a critical grain size, we can no longer use the concept of a pile-up to explain the plastic flow.

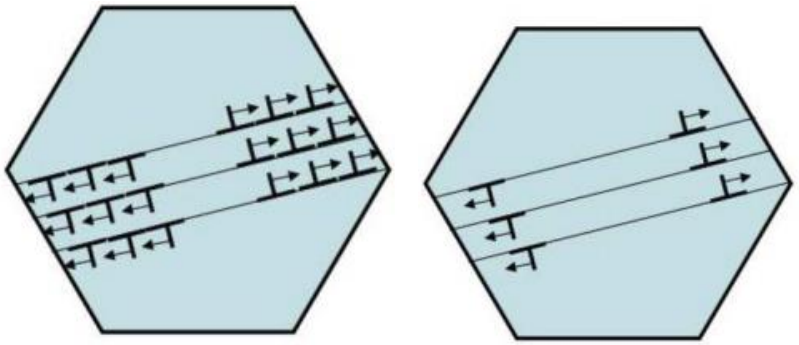

(a) (b)

Fig. 1.3 Breakup of dislocation pile ups: (a) microcrystalline regime and (b) nanocrystalline regime [2]

- **Grain boundary sliding:** The phenomenon of superplasticity has led to detailed study of grain-boundary sliding as the dominant deformation mechanism.Fig.1.4 shows a schematic in which one layer of grains slides with respect to the other, producing a shear strain in the process.

  Plastic deformation has taken place by virtue of the top layer of grains translating to the right with respect to the bottom layer of grains. This requires grain-boundary sliding and is the principal mechanism in superplasticity. For nanocrystalline materials, this has been proposed to be the dominant deformation mechanism at grain sizes <50 nm.

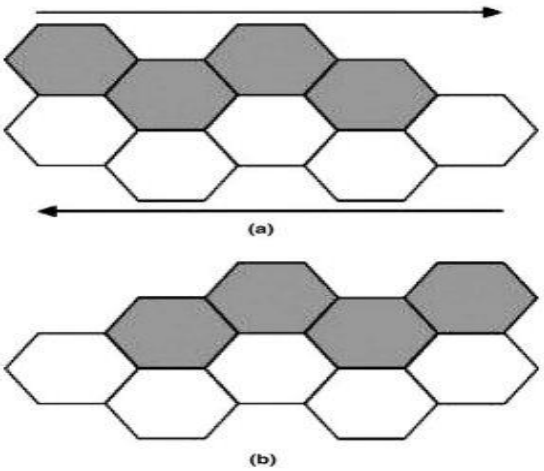

Fig. 1.4. Grain Boundary Sliding Model: (a) Initial Position of Grains (b) position after top layer has slide to right [2]

- **Core and mantle models:** In 1963, Li proposed that grain-boundary ledges acted as sources of dislocations at the onset of plastic deformation and that these dislocations created, by a double slip mechanism, a work hardened layer around the grain boundaries. This concept was later extended by Ashby who proposed that geometrically necessary and statistically stored dislocations were involved in polycrystalline deformation.

  The deformation within a grain is composed of two parts:

  (i) the core, or grain interior, which is subjected to a more homogeneous state of stress and (ii) the mantle, or grain-boundary region, in which several factors contribute to increased resistance to plastic flow and work hardening;grain boundary sources, change in orientation in the plane of maximum shear, elastic and plastic incompatibility.

- **Grain boundary rotation/grain coalescence:** Ma and coworkers point out the interesting possibility, that nanosized grains rotate during plastic deformation and can coalesce along directions of shear, creating larger paths for dislocation movement.Fig. 1.5 shows this in schematic fashion. The orientations of the slip systems with highest Schmid factors are represented by a short line in each grain (Fig.1.5(a)). As plastic deformation takes place, two neighboring grains might rotate in a fashion that brings their orientation closer together (Fig.1.5(b)).

This leads to the elimination of the barrier presented by the bound-ary between them, providing a path for more extended dislocation motion (Fig.1.5(c)). This mechanism can actually lead to softening and localization, and is consistent with the limited ductility often exhibited by nanocrystalline metals. One way by which grains can rotate is by disclinationmotion. Murayama & others first observed disclinations in a mechanically milled Fe sample and suggested that the generation of partial disclination defects provides an alternative mechanism to grainboundary sliding, which possibly allows rotation of nanosized crystals during mechanical milling.

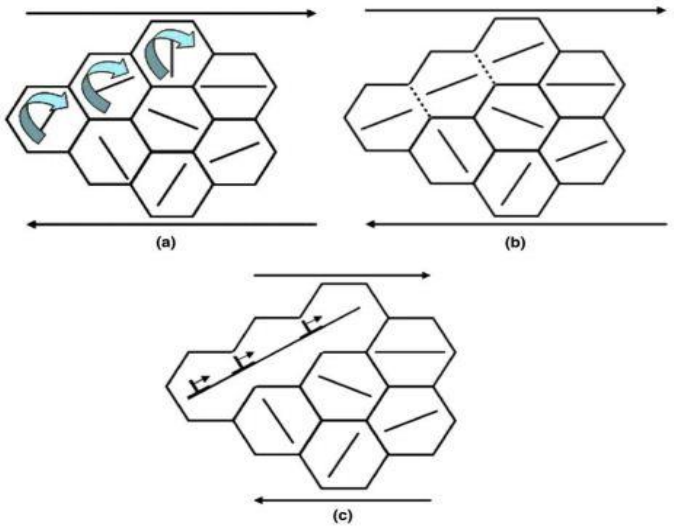

Fig.1.5. Rotation of neighboring nano grains during plastic deformation and creation of elongated grains by annihilation of grain boundary [2].

❖ **Shear band formation:** The deformation mode of nanocrystalline materials is known to change as the grain size decreases into the ultrafine regime. For all smaller grain sizes (d< 300 nm) shear band development is often observed to occur immediately after the onset of plastic deformation. Shear bands have been observed by Wei and others in both low and high strain rate tests. It was observed that under dynamic loading, conventional polycrystalline iron did not exhibit localized deformation. Fig. 1.6 compares the low-rate compressive deformation response of iron with two different grain sizes in the ultrafine grain size regime.

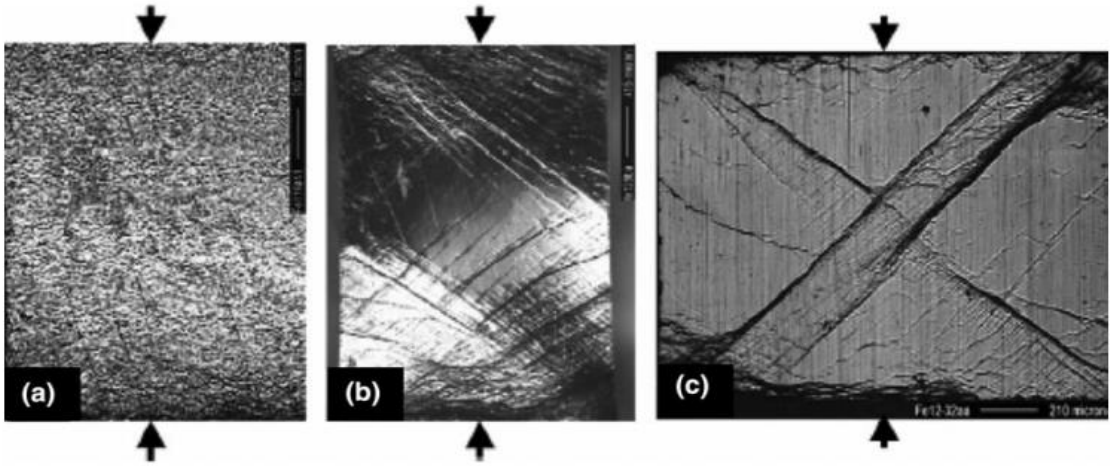

Fig.1.6. Change in deformation mode of ultrafine grained consolidated iron with grain size for uniaxial compression: (a) uniform low-rate deformation with d= 980 nm, e= 13.7%; (b) non-uniform low-rate deformation with d= 268 nm and (c) non-uniform high-rate deformation with d= 268 nm; Loading axis is vertical. [2]

❖ **Gradient models:** In conventional constitutive models, the stress is considered to be a function of strain, strain rate, and temperature. In gradient models, the stress is also assumed to be a function of the gradient of a variable. This gradient has taken several forms, depending on the researcher.

In any case, the gradient introduces a spatial scale into the constitutive description. This length scale has been successfully used to describe the effect of grain size, all the way from the nanocrystalline to the monocrystalline domains, into the calculation of the strength. An attractive approach to the analytical prediction of the grain size dependence is through strain-gradient plasticity. Strain gradient plasticity is a recent development that incorporates a length scale in the analytical treatment of plasticity problems. It enables the prediction of the effect of indentation size on the hardness of metals and ceramics, the effect of hard particles in the work hardening of metals, grain size and other effects.

- **Twinning**: Two types of twins are considered here: mechanical and growth (or recrystallization, or annealing) twins. In mechanical twins several processes of plastic deformation involving grain boundaries are seen:

(i) Heterogeneous nucleation of twin lamellae from the grain boundaries.
(ii) Homogeneous nucleation of twin lamellae from the grain interior.
(iii) Growth of twin lamellae to form a new grain.

Annealing resulted in a mixture of coarse and fine grained microstructure. The authors suggest that the excellent combination of strength and ductility is the result of (i) multi-axial stress states in the confined grains, (ii) growth twins in the larger grains, and (iii) preferential accommodation of strain in the larger grains. The grain size distribution allows for significant strain hardening which prevents localized deformation and premature fracture.

❖ **Grain boundary dislocation creation and annihilation:** Prompted by molecular dynamics simulations carried out primarily by Van Swygenhoven and coworkers and by TEM observations showing a low dislocation density after appreciable plastic deformation, a combined grain boundary source sink model is evolving. When the grain size is reduced to the nanocrystalline regime, the mean free path of dislocations generated at grain boundary sources is severely limited. Rather than cross slipping and generating work hardening, these dislocations can run freely until they meet the opposing grain boundary, which acts as a sink. Thus, the dislocation density remains low throughout the plastic deformation process, and work hardening is not significant which were generated at one grain boundary, run unimpeded until they encounter the opposing grain boundary. However, as the grain size falls below 20 nm, the grain boundaries will become virtually free of ledges, and intrinsic and extrinsic grain boundary dislocations have to be ‘‘pushed out’’ into the grains. Another significant difference is that the mean free path of dislocations is limited by the grain size, and therefore dislocation reactions, cross slip, and other mechanisms of dislocation multiplication are effectively prohibited.

1.6. Role of Computational Approach in Metallic Nanowires:

Today computational approach has gained popularity in studying numerous aspects of metallic nanowires because of the following reasons:

- Through computational approach, we can study both macroscopic and microscopic aspects of deformation of metallic nanowires e.g. atomistic level analysis can be done starting from crack initiation to fracture and also we can see the structural changes like development of voids which is not so clearly seen in laboratory experiments.

- Here, everything is analyzed by using proper software through computation which saves time and energy.
- Sometimes deformation of metallic nanowires is to be done at very high strain rate and at different temperatures which is difficult to achieve practically, but they can be analyzed through simulation.

Therefore, our main objective in this project work is to study the deformation behavior of Nickel Nanowire through molecular dynamics simulation studies.

1 .7 Properties of nanowires [1]:

- Nanowires are very strong, able to support tensions up to 1 nN.
- They are nearly-ideal one-dimensional conductors, and exhibit dramatically-reduced shot noise.
- Metallic Nanowires have high electrical and thermal conductance more than amorphous materials [4].

1.8 Applications of nanowires [1]:

- Nanowires may replace carbon nanotubes in some applications. They can be used to build the next generation of computing devices.
- To create active electronic elements by chemically doping a semiconductor nanowire.

- Conducting nanowires offer the possibility of connecting molecular-scale entities in a molecular computer.
- Dispersions of conducting nanowires in different polymers are being investigated for use as transparent electrodes for flexible flat-screen displays.
- Because of high Young's moduli, they are used in enhancing mechanical properties of composites.
- Because of their high aspect ratio, nanowires are also uniquely suited to dielectrophoretic manipulation.

Chapter-2

Literature Review

2.LiteratureReview:

T. DUÈ MMER[1], J. C. LASALVIA[2], G. RAVICHANDRAN[3] and M. A. MEYERS[4] [5] have studied effects of strain rate on plastic flow and failure in polycrystalline tungsten (< 100 p.p.m. impurities). Polycrystalline tungsten was subjected to different heat treatments to yield different grain morphologies and tested at quasi-static ($3x10^{-3}$/s) and dynamic (10^{3}- $4x10^{3}$/s) strain rates. Mechanisms of deformation were identified and evaluated as slip, twinning, and inter-granular cracking. Whereas plastic flow by slip has considerable strain-rate sensitivity in tungsten, the cohesive strength of the grain boundaries was found to decrease with heat treatment temperature, but was insensitive to any change in strain-rate. Deformation low-strain-rate yielded limited damage at strains as high as 0.25, whereas deformation at high-strain-rate led to catastrophic failure at strains ranging between 0.05 and 0.10. Slip and grain-boundary decohesion were competing deformation mechanisms and the material underwent a ductile-to-brittle transition as the strain rate was increased from 10^{-3} to 10^{3} /s. Two failure modes were identified: debonding initiated by shear along a grain-boundary and debonding initiated at voids. The interactions between twins and microcracks were characterized and there were evidences of fracture initiation at twins (intergranular cracks), and twin initiation at cracks (transgranular-cracks)

Hideyuki Ikeda, Yue Qi, Tahir Çagin, Konrad Samwer, William L. Johnson and William A. Goddard III [6] have studied the initial stage of plastic deformation behavior of metallic nanowire of pure nickel, using molecular dynamics methods.
In these simulations, they applied uniform strain along c-axis at strain rate of 0.5%/100ps, 0.5%/10ps and 0.1%/2ps. They observed the formation of stacking faults by movement of a partial dislocation and development of stacking faults to deformation twins at initial down event of stress-strain curve. Since twinning was also seen in at the slowest strain rate in their simulations, the twinning seemed to be a characteristic of deformation mechanism in metallic

nanowires.

Paulo S. Branicio and Jose-Pedro Rino [7] have done molecular dynamics study on Large deformation and amorphization of Ni nanowires under uniaxial strain. Molecular-dynamics simulations were employed to study deformations on nickel nanowires subjected to uniaxial strain at 300 K. Strong influence was observed in the Young modulus and force constant due to surface effects when considering nanowires with different cross sections. Applying strain rates from 0.05 % to 15 % ps^{-1}, they found elastic behavior up to 11.5% strain with corresponding stress of 9.4 GPa. At low strain rates (< 0.05% ps^{-1}) the system passes through plastic deformations although keeping the crystalline structure. At this low strain rate regime they observed that the nanowires show superplasticity. For high strain rates (>7% ps^{-1}) the system changed continuously from crystalline to amorphous phase. Although this amorphization occurred with no use of liquid quenching or introduction of chemical or physical disorder, so being a different process, the amorphous resulted was unstable. They studied this instability monitoring the recrystallization process.

R. Komanduri, N. Chandrasekaran, L.M. Raff [8] have done Molecular dynamics (MD) simulation of uniaxial tension of some single-crystal cubic metals at nanolevel. Molecular Dynamics (MD) simulations of uniaxial tension at nanolevel was carried out at a constant rate of loading (500 ms^{-1}) on some single-crystal cubic metals, FCC (Al, Cu, and Ni) and BCC (Fe, Cr, and W) to investigate the nature of deformation and fracture. Failure of the work materials due to void formation, their coalescence to form nanocracks and subsequent fracture were observed similar to their behavior at macroscale. Engineering stress-strain diagrams obtained by the MD simulations of the tensile specimens of various materials showed a rapid increase in stress up to a maximum followed by a gradual drop to zero when the specimen fails by ductile fracture. The radius of the neck was found to increase with an increase in the deformation of the specimen and decreased as the ductility of the material decreased. In

this investigation, the strain to fracture was observed to be lower with the BCC materials than FCC materials. No distinct linear trend in the engineering stress–strain characteristics was observed in the case of BCC crystals. Instead, rapid fluctuations in the force values were observed.

W Liang and **M Zhou** [9] have studied response of copper nanowires in dynamic tensile deformation. Molecular dynamics (MD) simulations were carried out to analyze the size and strain rate effects in the tensile deformation of single-crystal copper nanowires. The cross-sections of the wires were squares with dimensions of between 5 and 20 lattice constants. Deformations under constant strain rates between 1.67×10^{7} and $1.67 \times 10^{10} s^{-1}$ are analyzed. They found that the Yield stress decreased with specimen size and increased with loading rate. On the other hand, ductility increased with specimen size and strain rate. The influence of specimen size was due to enhanced opportunities for dislocation motion at larger sizes and the influence of strain rate was due to the dynamic wave effect or phonon drag which impedes the motion of dislocations. The analysis also focused on the variation in deformation mechanisms with specimen size and strain rate. Slip along alternating (111) planes was observed in small wires, while multiple cross-slips were primarily responsible for the progression of plastic deformation in larger wires. As strain rate was increased, a transition of the deformation mechanism from sequential propagation of slip along well defined and favourably oriented slip planes to cross slip and then **Yu-Hua Wen, Zi-Zhong Zhua, Gui-Fang Shao, Ru-Zeng Zhu [10]** have done atomic-scale computer simulations of uniaxial tensile deformation of Ni nanowire. The mechanical deformations of nickel nanowire subjected to uniaxial tensile strain at 300K were simulated by using molecular dynamics Simulations. For the strain rate of 0.1%/ps, the elastic limit was up to about 11% strain with the yield stress of 8.6 GPa. At the elastic stage, deformation was carried mainly through the uniform elongation of the distances between the layers

(perpendicular to the Z-axis) while the atomic structure remained basically unchanged With further strain, the slips in the {1 1 1} planes started to take place in order to accommodate the applied strain to carry the deformation partially and subsequently the neck formed. The atomic rearrangements in the neck region resulted in a zigzag change in the stress–strain curve. With the strain close to the point of the breaking, formation of a one-atom thick necklace in Ni nanowire was observed. It was concluded that strain rates have no significant effect on the deformation mechanism, but have some influence on the elastic limit, the yield stress **S. J. A. Koh, H. P. Lee, C. Lu and Q. H. Cheng [11]** have studied temperature and strain-rate effects in uniaxial tensile strain of a solid platinum nanowire through Molecular dynamics simulation. Their study focused on the molecular dynamics (MD) simulation of an infinitely long, cylindrical platinum nanowire (diameter 1.4 nm). The nanowire was subjected to uniaxial tensile strain along the [001] axis. The changes in crystal structure during deformation were analyzed and its mechanical properties were deduced from the simulation. MD simulation was employed in this study. The nanowire was subjected to strain rates of 0.04%, 0.4%, and 4.0% ps^{-1}, at simulation temperatures of 50 K and 300 K, in order to study the effects of different strain rates and thermal conditions on the deformation characteristics and mechanical properties of the nanowire. They found that the stress-strain response of the nanowire showed periodic, stepwise dislocation-relaxation recrystallization behavior at low temperature and strain rate, where crystal order and stability was high. The onset of amorphous crystal deformation occurred at 0.4% ps^{-1}, and fully amorphous deformation took place at 4.0% ps^{-1}, with amorphous melting detected at 300 K. Because of higher entropy of the nanowire at higher temperature and strain rate, periodic stress strain behaviour became less clearly defined and superplasticity behaviour was observed. This characteristic was significantly increased due to the development of a single-walled helical substructure at 300 K, when the nanowire was deformed at a lower strain rate. And the Young's modulus was found to be about 50% to 75%

that of its bulk counterpart, while there was no significant change in the Poisson ratio at the nanoscale.

S J A Koh and H P Lee [12] have studied Molecular dynamics simulation of size and strain rate dependent mechanical response of FCC metallic nanowires. The simulation scale was upped to 24,000 atoms to study a larger metallic nanowire with a 6 nm characteristic size scale. Au nanowire was studied in conjunction with Pt nanowire. The size and strain rate effects on the stretching behaviour of these nanowires were investigated through the simulation of nanowires with three different sizes of 2, 4 and 6 nm, subjected to three distinct strain rates of 4.0×10^{8}, 4.0×10^{9} and 4.0×10^{10} s^{-1}. These strain rates produce three distinct modes of deformation: crystalline-ordered deformation, mixed-mode deformation and amorphous disorder respectively. The mechanisms behind the observations of these distinct deformation modes were analyzed and explained. A Doppler 'red-shift' effect was observed when the nanowires were strained at the highest strain rate of 4.0×10^{10} s^{-1}. This effect was most pronounced for the nanowire subjected to the largest stretch velocity. A constrained dynamic free-vibration phenomenon was observed during stretching, which eventually led to delocalized multiple necking(s), instead of a single localized neck when it was strained at a lower rate.

Chapter-3

Computational Methods

3.1Modeling and Simulation[3]:

Model: When a system at some particular point in time or space simplified represent to promote understanding of the real system is called model.

Simulation: Simulation is the manipulation of a model. Simulation operates the model in such a way that it operates on time or space to compress it & it enables one to beware of the interactions that would not otherwise be apparent because of their separation in time or space.

Types of models: Based on the length scale there are 3 types of models:

(i) Atomistic

(ii) Monte carlo

(iii) Continuum

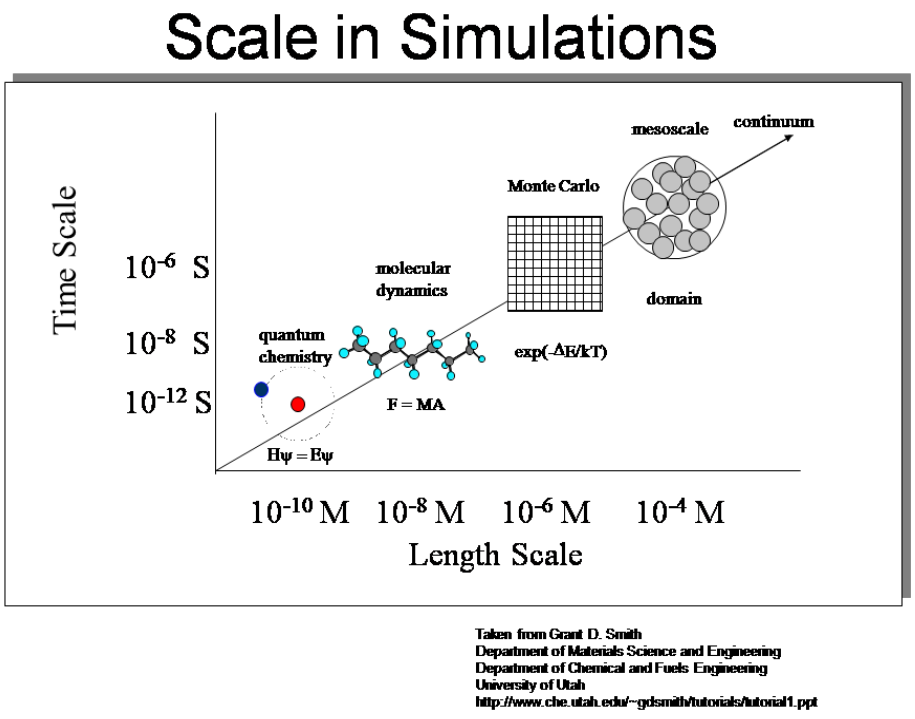

Fig.3.1 Time Scale vs. Length Scale [14]

Atomistic Modeling:

- At the level of atoms classified atomistic simulation models materials into two categories. They are Molecular statics and Molecular dynamics.
- In Molecular statics the relaxed configuration (positions and velocities) of atoms is found by conjugate gradient method or some similar energy minimization method. These simulations provide information of crystal lattice structure in different phases and under different conditions.

3.2Molecular dynamics simulation:

3.2.1 Introduction to MD simulations:

The actual motion of atoms is simulated by evolving the atomic configuration (atomic positions and velocities) with time by integrating Newton's Equation of Motion.

$$F = ma$$

Where 'a' is the acceleration & m is the mass of the particle. In a system atom and molecules are allowed to interact with each other for a long time with respect to their velocities and motion. By numerically solving Newton's equations of motion we can find out the trajectories of the interacting particles where potential energy and forces between the particles are defined by molecular mechanics force fields. The Newton's equation of motion in mathematically:

$$F=M_jA_j \quad \text{..... (I)}$$

$$A_j=d^2R_j/dt^2 \quad \text{..... (II)}$$

Where, F= force between the interacting particles,

A_j = Acceleration of each particle, M_j= mass of each particle,

R_j= particle position.

The subsequent time through which the particle movement &interaction takes place can be completely determined in a given initial set of velocities & positions.

During simulation atoms and molecules will move in the computer, hence subsequent changes will be there like:

- If constrained bumping into each other during interaction vibrating about a mean position .
- If the system is fluid wandering around, oscillating in waves in concert with their neighbors.
- Evaporating away from the system if there is a free surface.

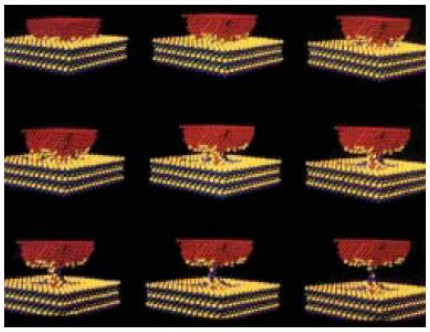

Fig. 3.2. MD simulation of nano-indentation of Au layer with Ni indenter [14].

In the late 1950s molecular dynamics was originally conceived within theoretical physics but is applied today mostly in materials science, chemical physics and the modeling of biomolecules.

Analytically it is impossible to find the properties of such complex systems, because molecular systems consist of a vast number of particles; MD simulations find a way out of this problem by using numerical methods. Cumulative errors can be generates in numerical integration by long MD simulations, because they are mathematically ill-conditioned. These errors can be suppressed by selecting proper algorithms & parameters.

3.2.2 Mechanism and design constraints: The study on the dynamics of molecules facilitates by MD simulations. By MD a trajectory is obtained as algorithm gives a set of conformations of molecule. Due to forces which act upon each & every atom; atoms & molecules interacts with each other. The forces originate from all other atoms by giving a certain initial momentum to all atoms and molecules. During movement positions & velocities of the atoms changes.

Typical on systems containing thousands of atoms MD simulations are performed. First initial positions and velocities are created for atoms. The initial positions usually correspond to a known structure (from NMR or X-ray structures). To initiate atomic movements & initial velocities are assigned taking them from a Maxwell distribution at a certain temperature T. Number of particles timestep, total time and simulation size duration must be selected so that the calculation can finish within a reasonable time period. Thermodynamic parameters of the system like pressure, volume, temperature & total energy changes as the simulation proceeds.

Simulation can be done in various ways. They are:

Microcanonical ensemble (NVE): In the microcanonical ensemble (NVE) there are changes in energy (E), volume (V) & moles (N).The system is isolated from those changes. With no heat exchange adiabatic process is corresponding to it. Exchange of kinetic and potential energy, with total energy being conserved, so microcanonical MD trajectory may be observed.

Canonical or NVT ensemble: In canonical or NVT ensemble conservation of temperature (T), Volume (V) and moles (M) occurs. It is a constant temperature MD simulation process. In NVT there is automatically regulation of temperature takes place and the energy of exothermic & endothermic process exchanged. Different types of thermostat methods are available to add and remove energy from the boundaries of molecular dynamics system in a more or less realistic way approximating the NVT ensemble.

Isothermal–Isobaric or NPT ensemble: In NPT ensemble conservation of temperature (T), volume (V) & moles (N) takes place. In addition to automatically temperature regulating device an automatically pressure maintaining device is needed.

Generalized ensembles: Generalized ensembles method is replica exchange method. Originally it was created to deal with the slow dynamics of irregular or disordered spin systems.

A MD simulation design should account for availability of computational power. Timestep, total time duration & simulation size must be selected properly so that the process can finish within a proper time period. Time span simulation should match the kinetics of the natural process for statistically valid conclusions from the simulations. Simulation time ranges from picoseconds to nanoseconds. For those simulations, several CPU-days to CPU-years are required. Parallel algorithms allow the load to be distributed among CPUs.

In classical molecular dynamics simulation, the important task of CPU is the evaluation of the potential as a function of internal coordinates of the particles.

This is the time length between evaluations of the potential. Total CPU time required by a simulation is the size of the integration timestep. To avoid discretization errors small timestep must be chosen that is smaller than the fastest vibrational frequency in the system. In MD simulation, how the particles in the simulation will interact measured quantitatively by potential function (force field). A classical treatment of particle-particle interactions represent by these potential functions. This results in structural and conformational changes but usually cannot reproduce chemical reactions.

3.2.3 Applications of MD simulation:

- It is used to examine the dynamics of atomic level phenomena that cannot be seen in naked eye for example thin film growth & ion sub plantation.
- It is used to examine the physical properties of nano-technological devices that have not or cannot yet be discovered.
- It is used in biophysics & biochemistry.
- It is used to examine the ion irradiation & effect of neutrons on the surface of solid.
- It is used to study various mechanical and physical properties of metals, nonmetals & alloys like tensile properties, fatigue properties, high temperature behavior deformation behavior, etc.

3.2.4 How does an MD simulation run ?

- First initialize the positions and velocities of the atoms.
- Calculate energy.

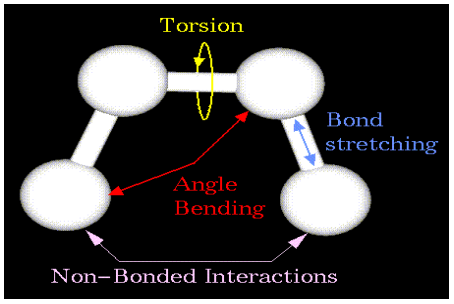

$E_{total}=E_{bond} + E_{bond\ angle} + E_{non\ bond} + E_{torsion}$

- Calculate the forces on the atoms.

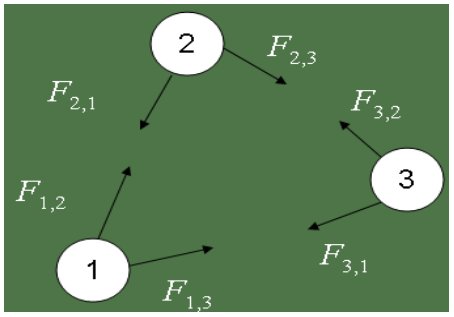

- Move the atoms and integrate Newton's equations of motion to obtain atomic trajectory.

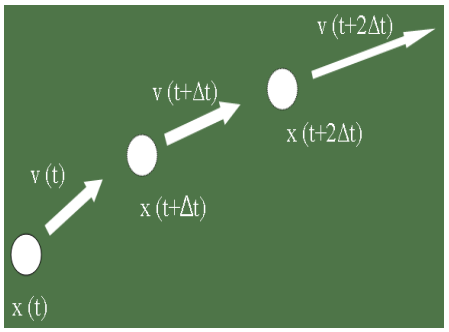

$$\vec{F} = m\vec{a} \qquad x(t+\Delta t) = x(t) + v_x(t)\Delta t + \frac{1}{2}a_x(t)(\Delta t)^2 \qquad v_i(t+\Delta t) = v_i(t) + a_i(t) \bullet \Delta t$$

- Numerical algorithms- Runge-Kutta method, Hamiltonian method for solving the differential equations. The most commonly used time integrator algorithm is Verlet algorithm.
- Update the new positions and velocities after timestep 0.001 ps (Δt).

Flow chart of typical MD code:

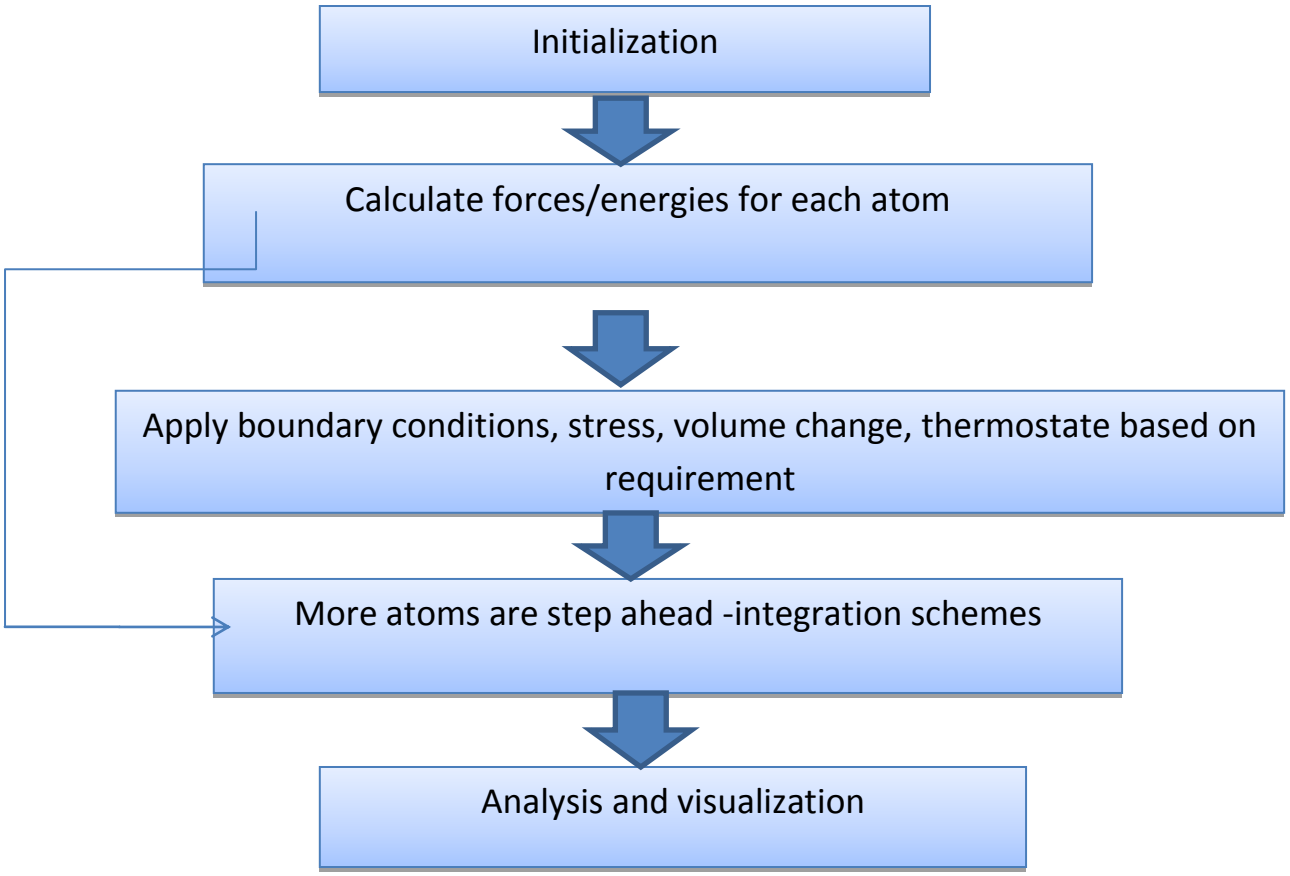

3.3 LAMMPS & VMD:

- LAMMPS stands for Large-scale Atomic/Molecular Massively Parallel Simulator. The LAMMPS was released in 1 May 2010. Since then, LAMMPS is updated continuously.
- LAMMPS is a classical MD simulation code designed to run effectively on parallel LAMMPS was developed at Sandia National Laboratories, a US Department of Energy facility, with funding from the DOE.
- For partition of simulation domain into small 3d sub-domains, LAMMPS uses one of the techniques which are assigned to each processor called spatial decomposition technique.
- In the systems whose particles fill a 3D rectangular block with approximately uniform density in a parallel computing sense LAMMPS is the most pronounced software.
- LAMMPS has potentials for many materials like solid state materials e.g. metals & semiconductors, soft materials e.g. polymers & biomolecules and coarse-grained systems. It can be used to model atoms or as a parallel particle simulator at the atomic, continuum or meso scale.
- A set of pre- and post-processing tools are also packaged with LAMMPS, which can convert input and output files to/from formats used by other codes.
- VMD (Visual Molecular Dynamics) is a molecular visualization program for displaying, analyzing & animating large molecular systems using 3-D graphics and built-in scripting. VMD also an open source code.
- VMD supports all computer processors, platforms and not limited by number of particles in the system except availability computer memory.

In this project work, LAMMPS code has been used for all the simulations and resulting structures & models have been analyzed using VMD.

Some metallurgical/mechanical studies on materials using LAMMPS:

- Melting and solidification
- Fracture
- Shear
- Tensile and compression
- Nano-indentation
- Viscosity
- Thermal conductivity
- LAMMPS can also be used for molecular modeling

3.4 Simulation Procedures:

3.4.1Input of simulation procedures:

- For simulation, first we have to install LAMMPS software in the computer.
- To run a simulation we need 3 programs. They are:
    - In .file (program file to create models and doing simulation)
    - Potential file(contains data about inter atomic bond energy between atoms)
    - Exe file (required to run the commands in the in .file)

To study deformation we need a data file containing prior atomic coordinates of the cylindrical structure.

- Then we have to open command prompt screen by typing "cmd" in start icon.
- In the displaying screen, the default directory will be displayed as "C:\users\name of the computer>" for ex: C:\users\hp>. If the above program files are in another directory, we have to change the path directory by typing in the screen as "C:\users\name of the computer>directory name: enter"(for ex: C:\users\hp>E:enter).Then the desired directory name will be displayed as "directory name :\>". (For ex: E :\>).
- Then type as E:\>cd "path address of the above program files in the LAMMPS folder" then press enter. Then the screen will display the same path address. After that next to the path address type as: "Path address > lmp_win_no-mpi.exe<in.file name" then press enter. Then automatically the in.file will be executed by the .exe file and if there is any error in the in.file then it will be displayed in the command prompt screen and after rectification of all the errors, the output values will be displayed.

3.4.2 Output of simulation procedures:

After successful running of the in.file, we will get four out-put files as follows:

- DUMP file (containing the atomic co-ordinates of the final structure after simulation and also for deformation studies it contains the stress component values).
- RDF file (contains co-ordination values of atoms and radial distribution function values). RDF or radial distribution function is a measure of arrangement of atoms in the material.
- Log file (contains thermodynamic data e.g. temperature, pressure, volume and total energy after a particular no of steps).

- Log. lammps file
- Now to see the final structure after simulation, we have to open dump file that contains atomic co-ordinates, through VMD software which need to be installed in the system.
- VMD has three parts:

    - VMD main
    - Display screen
    - Program screen

- Necessary adjustments to the final structure like change of colour, display format (Atomic or point) can be done through VMD main. In display screen we see the image of the final structure. In the program screen, any changes that we do in VMD main and final results are displayed.

Chapter-4

Results & Discussions

Simulations and analysis carried out during the execution of this project work are as follows:

(a) Creation of Nickel Nanowire models of different sizes (25 x 100) and (20 x 80) {diameter (Å**)** x height (Å)} in crystalline form.

(b) Creating read_data file which the co-ordinates of the atoms of the stable crystal and this file is created from the data in last iteration step of dump file obtained after simulation.

(c) Uniaxial tensile deformation of Nanowires along y-direction under controlled temperatures conditions strain rates ranging from 1 x 10^9 – 3 x 10^{11} with 40 % strains at different temperatures of 50 K, 100 k, 300 k and 500k.

(d) Strain corresponding to stress was calculated and Stress vs. Strain Graphs were plotted to find various mechanical properties; ultimate tensile strength, rupture stress, Elastic Modulus, First Yield Stress.

4.1 Creation of Nickel nanowire models:

Here the aim of simulation is to create a Nickel Nanowire model e.g. a crystalline structure at room temperature.

.The in.file which contains all the commands to create a Nickel Nanowire model is given below:

 # In.file (for Nickel Nanowire size diameter = 25 Å, height =100 Å):

```
units           metal
Echo            both
atom_style      atomic
Dimension       3
Boundary        p p p
region          mycylinder cylinder y 0 0 25 0 100 units box
create_box      1 mycylinder
lattice         fcc 3.52
region          Ni cylinder y 0 0 25 0 100 units box
create_atoms    1 region Ni units box
timestep        0.002
pair_style      eam
pair_coeff      * * Ni_u3.eam
# Energy Minimization
minimize        1.0e-4 1.0e-5 10000 10000
thermo          1
thermo_style    custom step temp vol press etotal pe ke
dump            1 all atom 100 Ni_crystal_3d_s_dump.lammpstrj
```

```
dump_modify          1 scale no

log logNi_crystal_3d_s.data

velocity             all create 500 873847 rot yes mom yes dist gaussian

#fixes

fix                  1 all npt temp 500 500 0.1 iso 0.0 0.0 0.1

run                  20000

unfix                1
```

Through this in.file named in.Ni (user defined) along with potential file for Ni which is named within the in.Ni file as Ni_u3.eam and lmp_win_no-mpi.exe file simulation can be done. For nanowires of other dimension, the in.file is modified by changing the dimensions in the region command.

After successful running, the crystalline Nickel nanowire models of different sizes are obtained which can be seen in VMD. The VMD images of the crystalline structures for different sizes are given below:

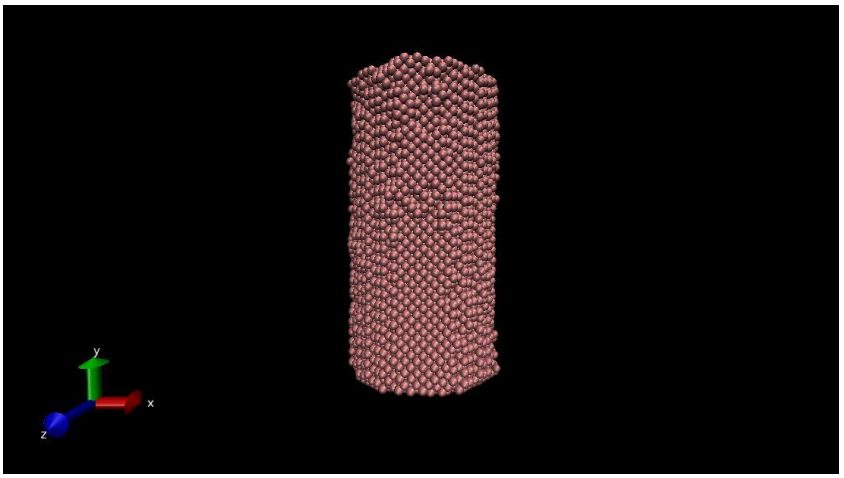

Fig. 4.1 VMD snap shot showing Nickel Nanowire model of Size:
diameter = 25 Å, height =100 Å, (No of atoms=18041)

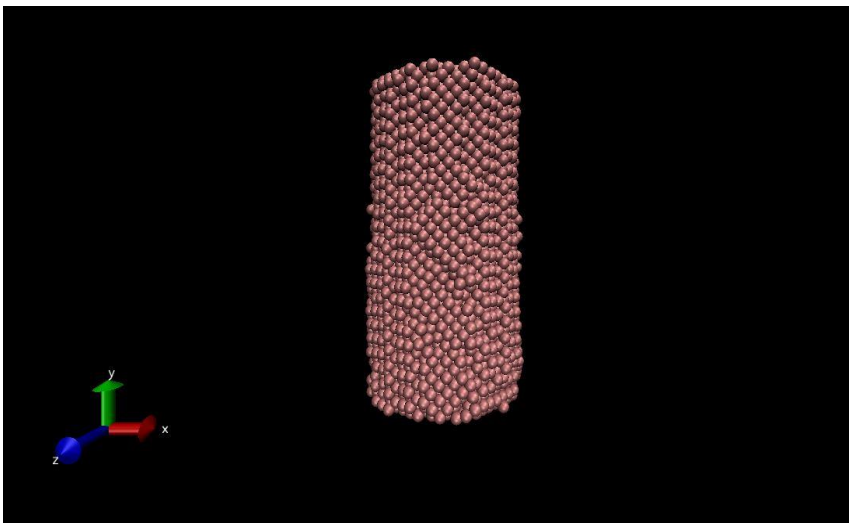

4.2 VMD snap shot showing Nickel Nanowire model of Size: diameter = 20 Å, height =80 Å (No of atoms=9315)

4.2 Tensile Deformation of Nickel nanowires:

Computational Steps:

(a) To run a tensile deformation simulation program 4 files are needed which are in.file, potential file, read_data file and lammps.exe file in a one folder.

(b) Read_data fie contains the co-ordinates of the atoms of the stable crystal and this file is created from the data in last iteration step of dump file obtained after simulation.

(c) Output files include dump file, dump.stress file, log file, log.lammps file.

(d) Dump.stress file gives six components of stress tensor which are in the order σ_x, σ_y, σ_z, τ_{xy}, τ_{xz}, τ_{yz} where only σ_y will be used to plot Stress vs Strain curve.

Here the objective of simulation is to do uniaxial tensile deformation of the nanowire along y-direction. Below is the in.file which contains all the commands required to do simulation of tensile deformation. First the deformation was carried out for different sizes at a particular strain rate, then for a particular size at different strain rates and after that for a particular size and particular strain rate at different temperatures. Then after Stress-strain plots were drawn to find various mechanical properties like ultimate tensile strength, rupture stress, Young's Modulus, first Yield Stress.

For deformation of different sizes at a particular strain rate and temperature, read data file was changed according to the size concerned by accessing the data in the dump file obtained after simulation. Similarly, to do deformation at different strain rates for same size the strain rate which is mentioned as 'erate' in the in.file was changed accordingly. Also, to do deformation at different temperatures at same strain rate and size, the temperature which is mentioned as 'temp' in the in.file was changed accordingly.

 # In.file for 3d tensile simulation (at strain rate 10^{11} s^{-1}):

```
Units           metal
Echo            both
atom_style      atomic
read_data       DATAFILE.txt
timestep        0.002

pair_style      eam
```

```
pair_coeff              * * Ni_u3.eam
# Energy Minimization
#minimize              1.0e-4 1.0e-5 10000 10000
dump   1 all atom 100 dump.JP4_tensile_review_10^11s-
1_40%strain_f1_allatoms.lammpstrj
 log                   log5050_JP4_review_10^11s-1_80%strain_f1_allatoms.dat
 # initial velocities
 velocity              all create 298 482748 rot yes mom yes dist gaussian
 fix                   1 all deform 1 y erate 0.1
 fix                   2 all npt temp 50.0 50.0 10.0 x 0 0 10.0 z 0 0 10.0   dilate all
 fix                   3 all temp/rescale 10 50 50 0.05 1.0
 compute               1 all stress/atom

 compute               2 all temp


 dump                  2 all custom 100
 dump.stress_atom_Jp4_review_10^11s1_40%strain_f1_allatoms type x y
  z c_1[1] c_1[2] c_1[3] c_1[4] c_1[5] c_1[6]
 compute               3 all reduce sum c_1[2]

 variable              stress equal c_3/(3*49062.50)

 variable              stress_GPa equal v_stress/10000
 thermo                      1
 thermo_style          custom step temp press vol etotal c_2 v_stress v_stress_GPa
 run                   2000
```

Structure of Ni Nanowire before and after tensile deformation:

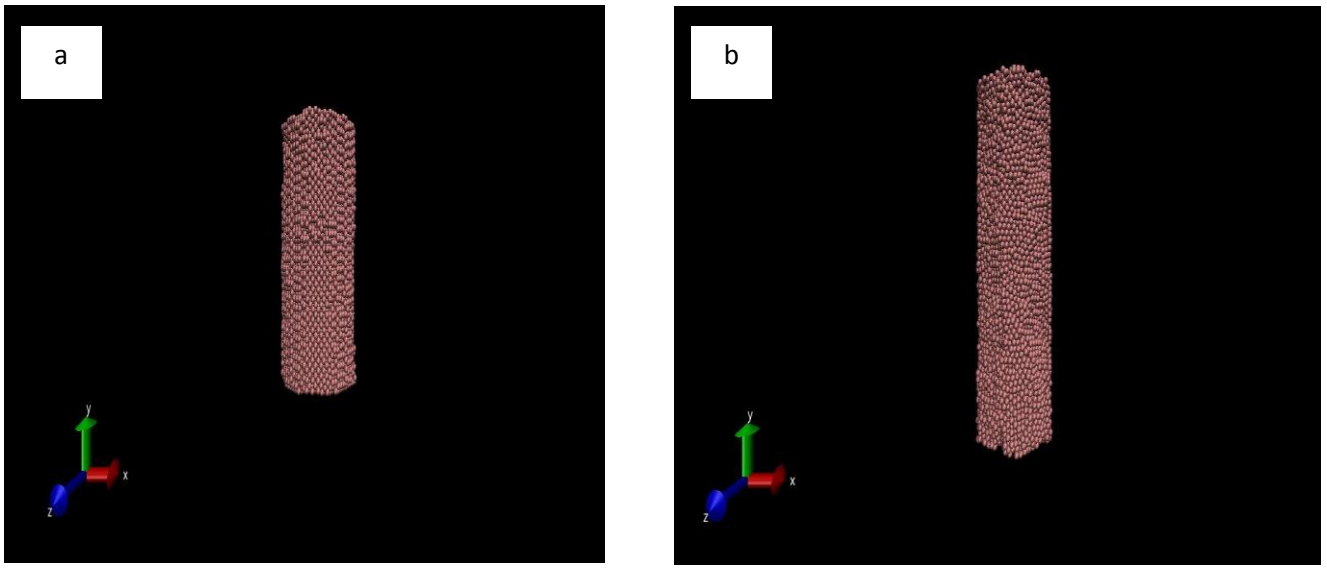

Fig. 4.3 Structure of Ni nanowire model before and after tensile deformation: (a) Structure of nanowire model before uniaxial tensile deformation; (b) Structure of nanowire model after uniaxial tensile deformation for 4 ps (size: diameter =20 Å, height =80 Å).

From the above figures, we can observe the change in the structure (since tensile deformation was done in y-direction, so dimension was increased in that direction).

Stress Strain Plots for different sizes of Ni nanowire at same strain rate 1 x 10^{11} s^{-1} at 50 K temperature:

Table 4.1: Stress-strain data for size diameter = 25 Å, height =100 Å (180451 atoms) at strain rate of 1 x $10^{11}s^{-1}$

Stress (GPa)	Strain
0.007073	0.00
8.458111	0.05
17.3845	0.10
23.06048	0.15
20.56576	0.20
16.65585	0.25
13.72579	0.30
11.91575	0.35
11.00202	0.40

Based on the data given in Table 4.1, the stress-strain plot obtained has been shown below:

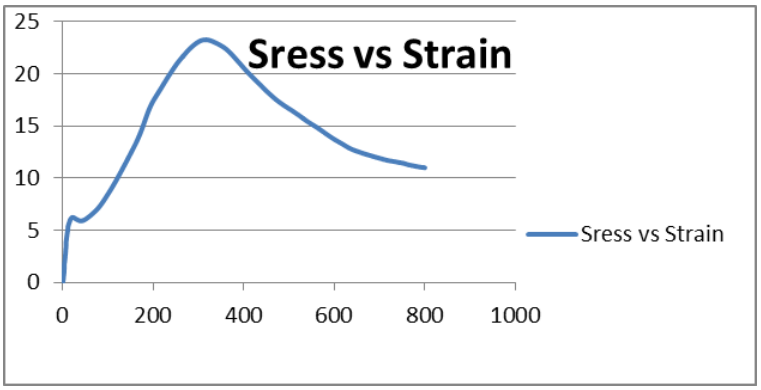

Fig.4.4: Engineering stress-engineering strain plot for size diameter = 25 Å, height=100 Å (180451 atoms) at strain rate of 10^{11} s^{-1}.

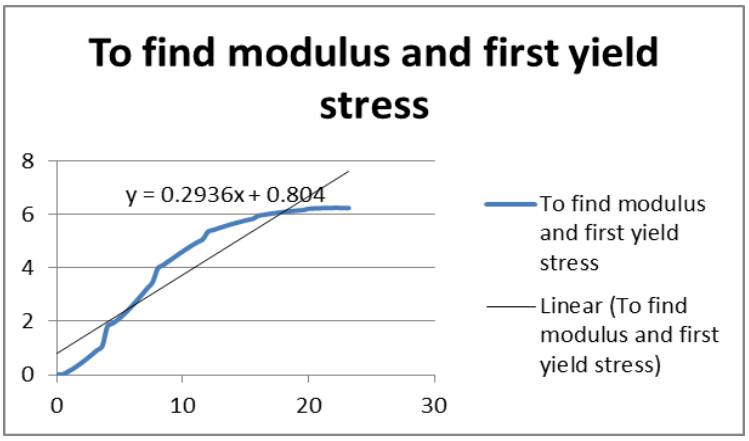

Fig.4.5: A part of graph 4.4 to find Elastic Modulus and first Yield Stress.

From the above graphs, we found different mechanical properties:

Mechanical Prop.	Value (GPa)
UTS (GPa)	22.63
Rupture Stress (GPa)	11.00
First Yield Stress (GPa)	6.243
Elastic Modulus (GPa)	0.299

Table 4.2: Stress-strain data for size diameter = 20 Å, height =80 Å (18041 atoms) at strain rate of 1 x 10^{11} s^{-1}

Stress (GPa)	Strain
0.00707	0.00
8.45811	0.05
17.38457	0.10
23.06048	0.15
20.56576	0.20
16.65585	0.25
13.72581	0.30
11.91575	0.35
11.00202	0.40

Based on the data given in Table 4.2, the stress-strain plot obtained has been shown below:

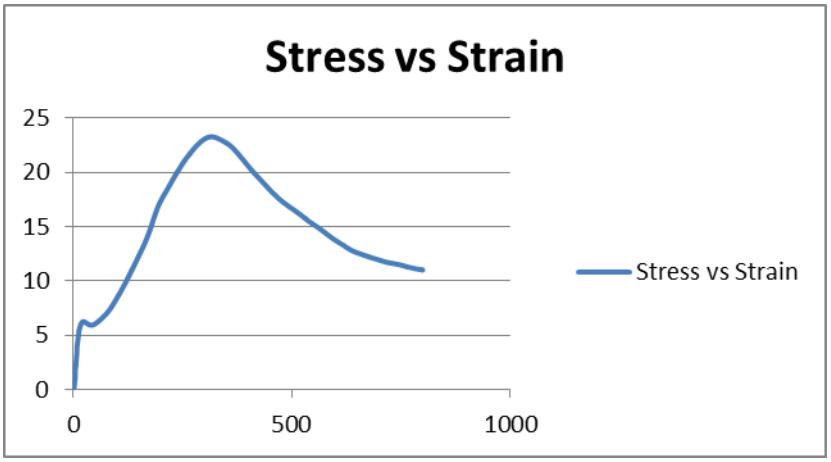

Fig. 4.6: Engineering stress-engineering strain plot for size diameter = 20 Å, height=80 Å (18041 atoms) at strain rate of 1 x 10^{11} s^{-1}.

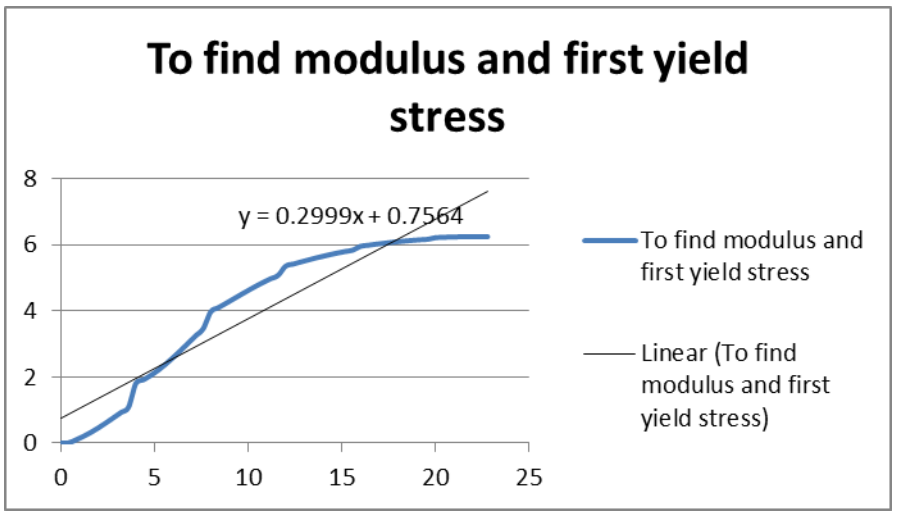

Fig. 4.7: A part of graph 4.6 to find Elastic Modulus and first Yield Stress.

From the above graphs, we found different mechanical properties:

Mechanical Prop.	Value (GPa)
UTS (GPa)	23.25667
Rupture Stress (GPa)	11.00202
First Yield Stress (GPa)	6.2433
Elastic Modulus (GPa)	0.299

Comparison of the stress-strain plots for deformation at different sizes a t a particular temperature of 50 k and strain rate 1x 10^{11} :

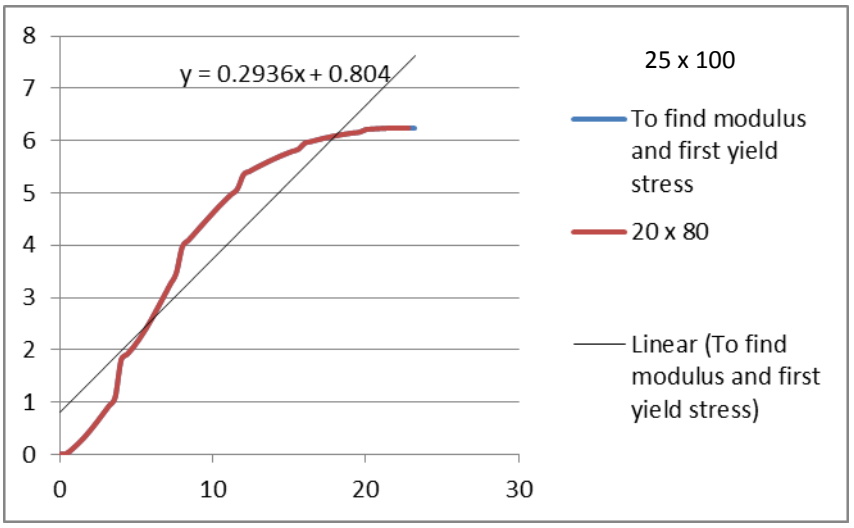

Fig. 4.8

From above figures and tables we conclude that the deformation behavior of nanowires with different size at same strain rate is almost similar [4]. The larger cross-sectional dimension leads to larger maximum yielding stress and larger cross-sectional dimension nanowires have less numerical oscillations amplitude compared to the smaller cross-sectional dimension nanowires [13].

Stress-Strain plots at different strain rates for size diameter = 20 Å, height =80 Å (18041 atoms) at 50 k temperature:

Table 4.3: Stress-strain data for size diameter = 20 Å, height =80 Å (18041 atoms) at strain rate of 1×10^{9} s^{-1}

Stress (GPa)	Strain
0.00707	0.00
7.26527	0.05
6.40884	0.01
4.05025	0.15
4.21311	0.20
5.31759	0.25
4.76769	0.30
6.13064	0.35
6.61896	0.40

Based on the data given in Table 4.3, the stress-strain plot obtained has been shown below:

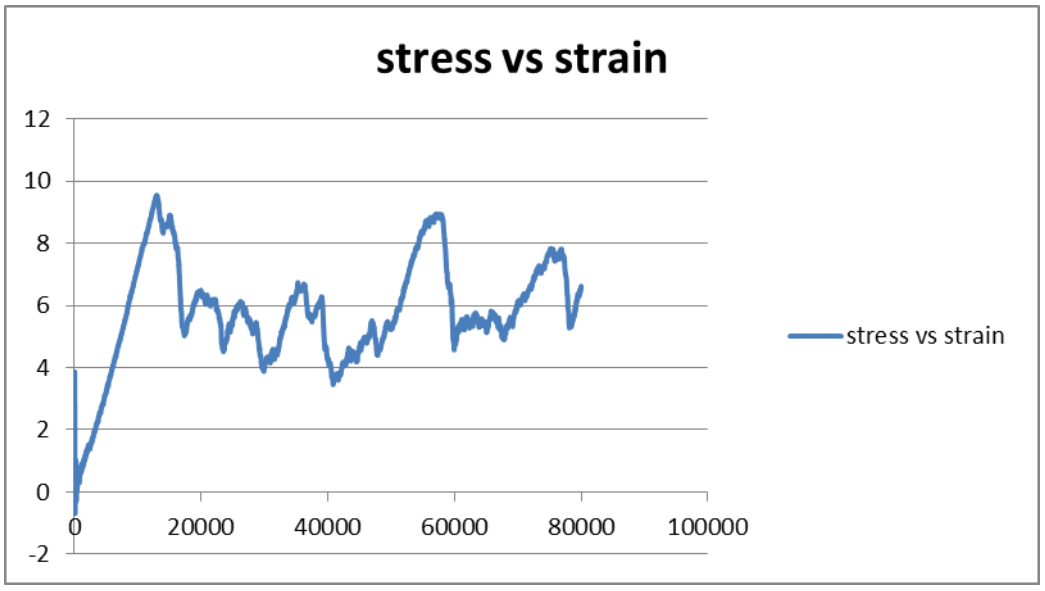

Fig. 4.9: Engineering stress-engineering strain plot for size diameter = 20 Å, height=80 Å (18041 atoms) deformed at strain rate of 1×10^{9} s^{-1}.

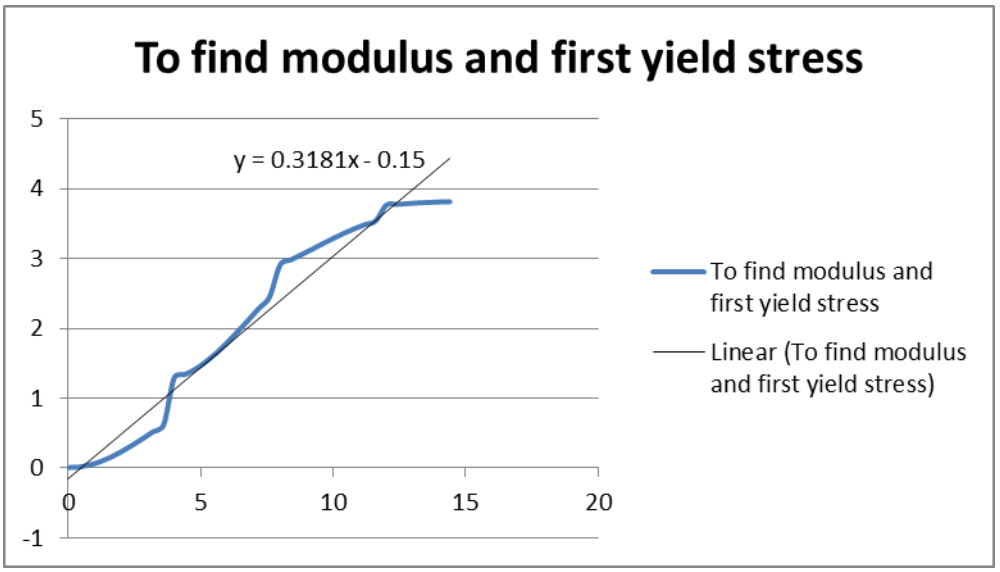

Fig. 4.10: A part of graph 4.9 to find Elastic Modulus and first Yield Stress.

From the above graphs, we found different mechanical properties:

Mechanical Prop.	Value (GPa)
UTS (GPa)	9.5420762
Rupture Stress (GPa)	6.618964
First Yield Stress (GPa)	3.8117
Elastic Modulus (GPa)	0.3181

Table 4.4: Stress-strain data for size diameter = 20 Å, height =80 Å (18041 atoms) at strain rate of 1 x 10^{10} s^{-1}

Stress (GPa)	Strain
0.00707	0.00
7.26529	0.05
10.16988	0.01
6.69935	0.15
8.98708	0.20
8.05610	0.25
6.85852	0.30
5.92454	0.35
7.01788	0.40

Based on the data given in Table 4.4, the stress-strain plot obtained has been shown below:

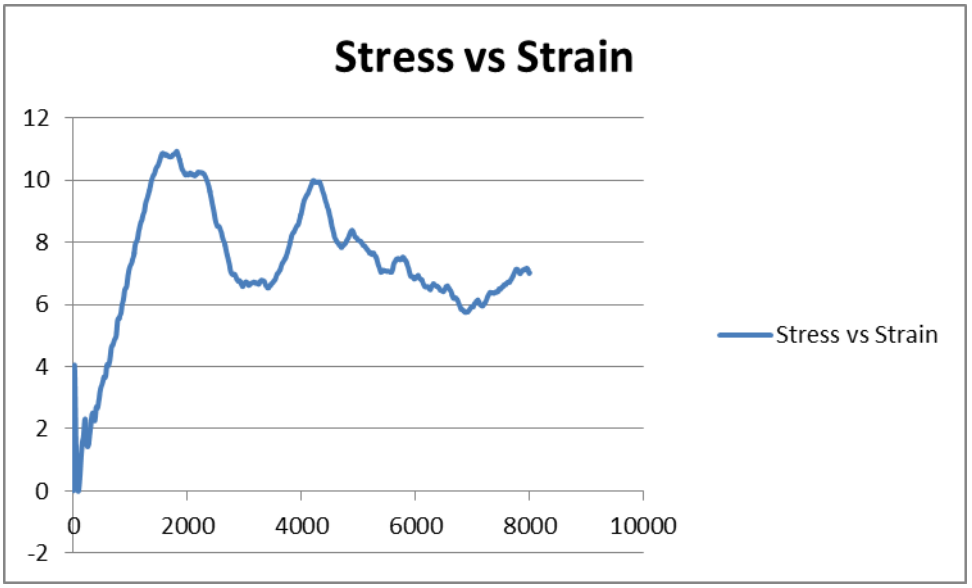

Fig. 4.11: Engineering stress-engineering strain plot for size diameter = 20 Å, height=80 Å (18041 atoms) deformed at strain rate of 1 x 10^{10} s^{-1}.

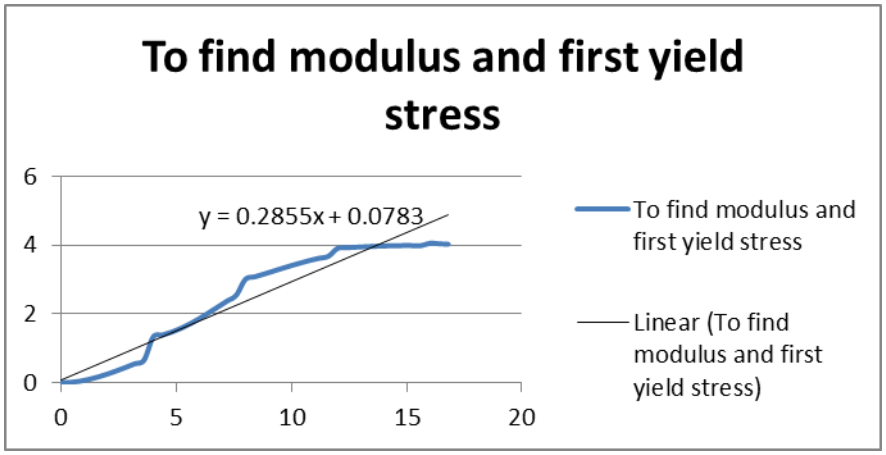

Fig. 4.12: A part of graph 4.11 to find Elastic Modulus and first Yield Stress.

From the above graphs, we found different mechanical properties:

Mechanical Prop.	Value (GPa)
UTS (GPa)	10.92827
Rupture Stress (GPa)	7.01788
First Yield Stress (GPa)	4.0554
Elastic Modulus (GPa)	0.2855

Table 4.5: Stress-strain data for size diameter = 20 Å, height =80 Å (18041 atoms) at strain rate of 1 x 10^{11} s^{-1}

Stress (GPa)	Strain
0.007074	0.00
8.458111	0.05
17.38457	0.01
23.06048	0.15
20.56576	0.20
16.65585	0.25
13.72581	0.30
11.91575	0.35
11.00202	0.40

Based on the data given in Table 4.5, the stress-strain plot obtained has been shown below:

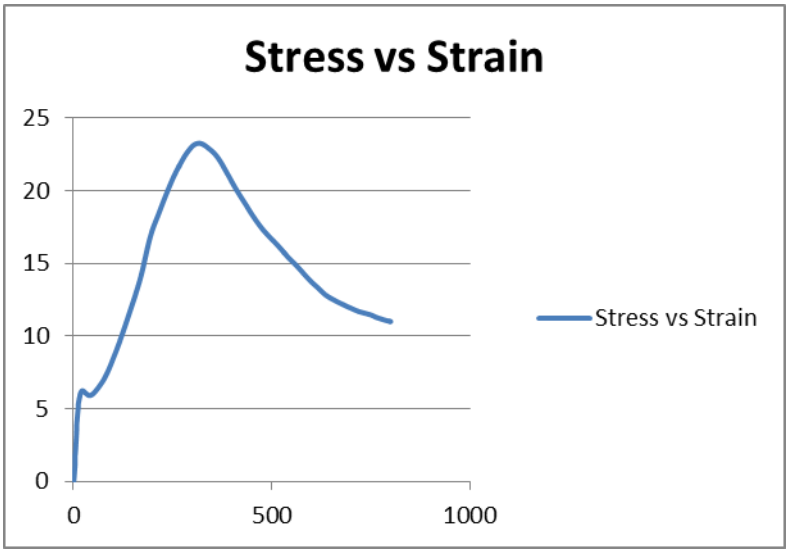

Fig. 4.13: Engineering stress-engineering strain plot for size diameter = 20 Å, height=80 Å (18041 atoms) deformed at strain rate of 1 x 10^{11} s^{-1}.

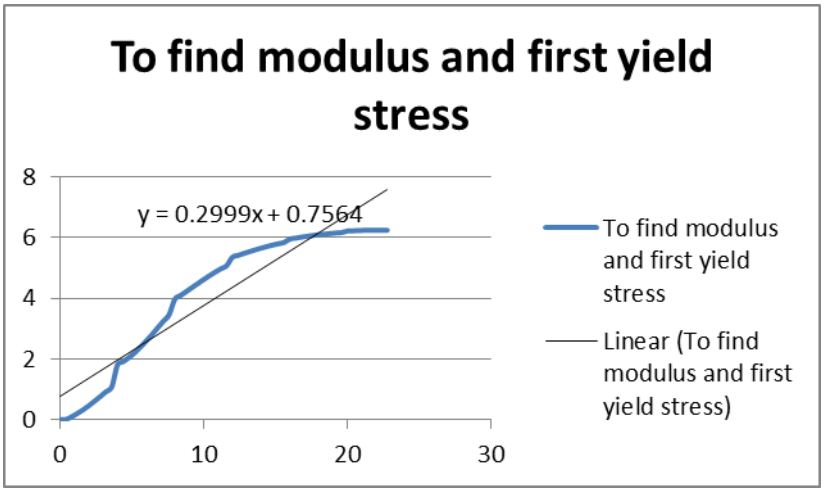

Fig.4.14: A part of graph 4.13 to find Elastic Modulus and first Yield Stress.

From the above graphs, we found different mechanical properties:

Mechanical Prop.	Value (GPa)
UTS (GPa)	23.25667
Rupture Stress (GPa)	11.00202
First Yield Stress (GPa)	6.2433
Elastic Modulus (GPa)	0.2999

Comparison of the stress-strain plots for deformation at different strain rates a t a particular temperature of 50 k and size (20x80):

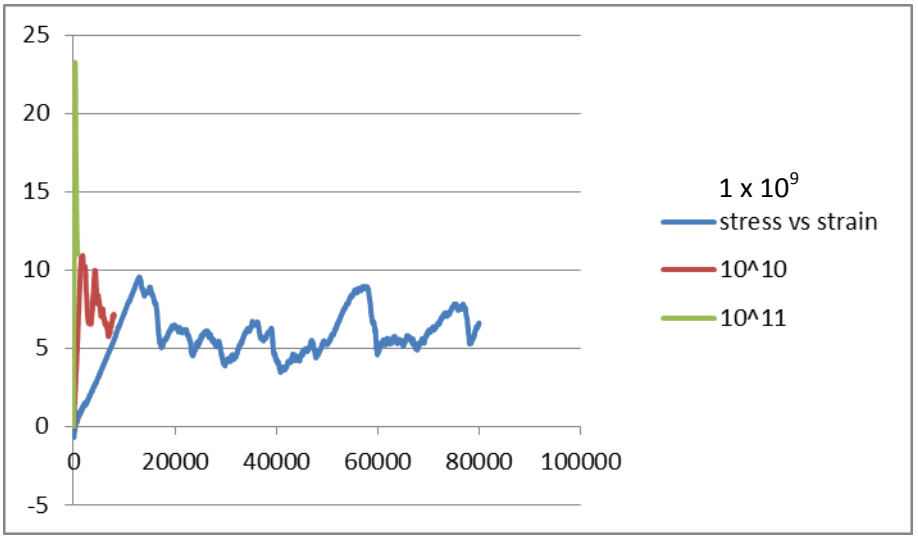

Fig 4.15

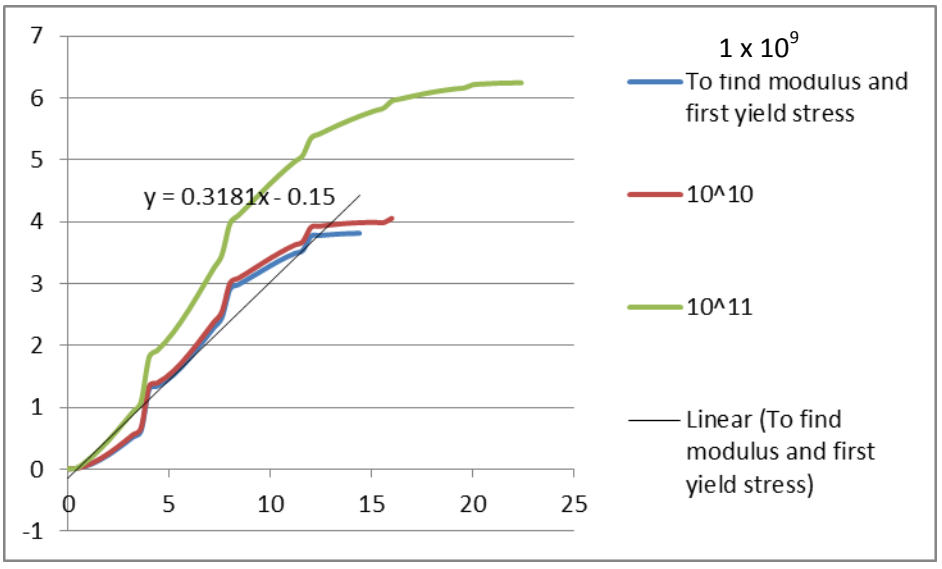

Fig 4.16

From the above figures & tables we conclude that at particular temperature as strain rate increases the UTS, rupture stress & first yield stress increases, but elastic modulus decreases.

The increase in strain rate increases the flow stress. However at higher strain rates of order of 10^{13} s^{-1} due to the formation of voids at the early stage of deformation there is sharp decrease in stress compared to the other strain rates [4].

The effect of strain rate is due to the dynamic wave effect or phonon drag which impedes the dislocation motion [13].

As the strain rate is increased, a transition of the deformation mechanism from sequential propagation of slip along well-defined & favorable oriented slip planes to amorphization is observed [13].

At higher strain rate of the order 10^{10} s^{-1}, momentum-induced disorder takes place. This disorder weakens the crystal structure & disrupts the discrete lattice order & the nanowire goes into a mixed-mode heterogeneous-homogeneous plastic flow deformation. Momentum-induced lattice disorder reduces the average cohesive energy by about 60 meV & hence encourages simultaneous formation of multiple dislocation planes in the crystallographically weakened nanowire [12].

Stress-Strain plots at particular strain rate deformed at different temperatures for size diameter = 20 Å, height =80 Å (18041 atoms):

Table 4.6: Stress-strain data for size diameter = 20 Å, height =80 Å (18041 atoms) at strain rate of 3 x $10^9 s^{-1}$ deformed at 50 K temperature:

Stress (GPa)	Strain
0.007078	0.00
6.410982	0.05
6.156065	0.01
4.541736	0.15
4.641834	0.20
4.905843	0.25
6.467751	0.30
5.125769	0.35
6.353541	0.40

Based on the data given in Table 4.6, the stress-strain plot obtained has been shown below:

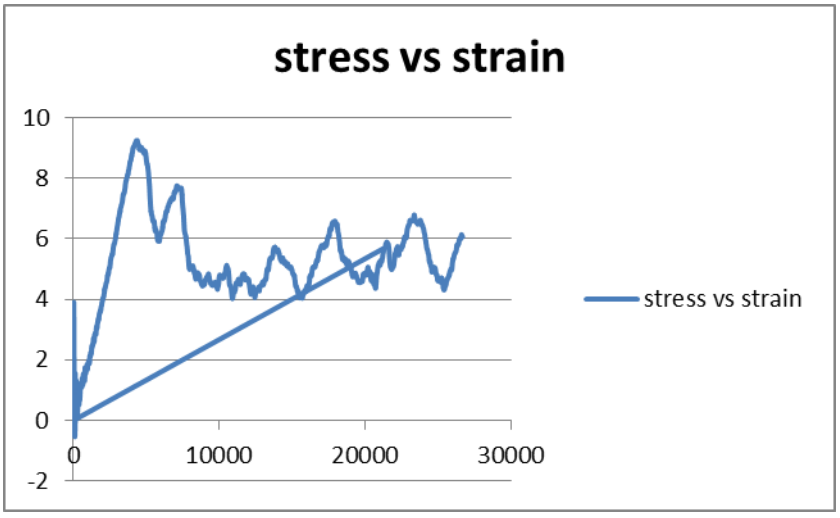

Fig. 4.17: Engineering stress-engineering strain plot for size diameter = 20 Å, height=80 Å (18041 atoms) at strain rate of 3 x 10^9 s^{-1} deformed at 50 K.

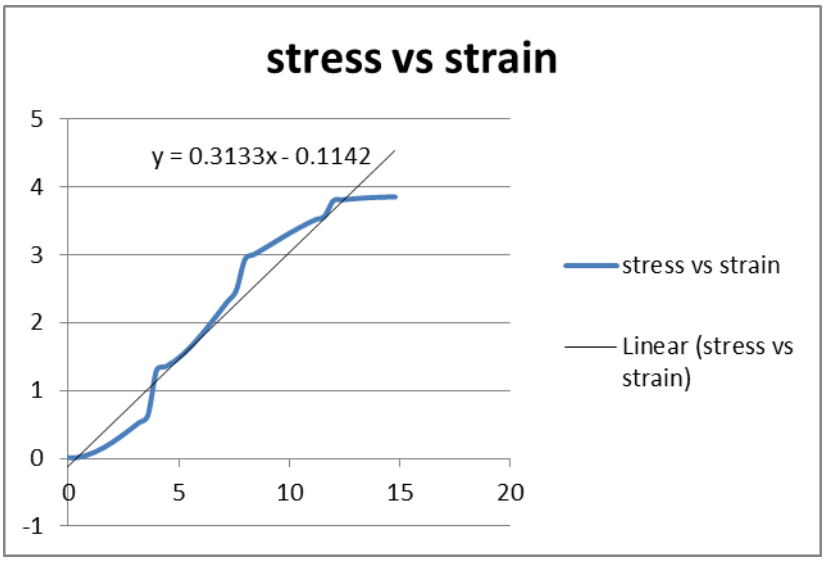

Fig. 4.18: A part of graph 4.17 to find Elastic Modulus and first Yield Stress.

From the above graphs, we found different mechanical properties:

Mechanical Prop.	Value (GPa)
UTS (GPa)	9.256607
Rupture Stress (GPa)	6.0642
First Yield Stress (GPa)	3.8505731
Elastic Modulus (GPa)	0.3133

Table 4.7: Stress-strain data for size diameter = 20 Å, height =80 Å (18041 atoms) at strain rate of 3 x $10^9 s^{-1}$ deformed at 100 K temperature:

Stress (GPa)	Strain
0.00707	0.00
6.16830	0.05
5.46719	0.01
6.06551	0.15
6.75121	0.20
6.10994	0.25
9.05086	0.30
8.37325	0.35
5.33007	0.40

Based on the data given in Table 4.7, the stress-strain plot obtained has been shown below:

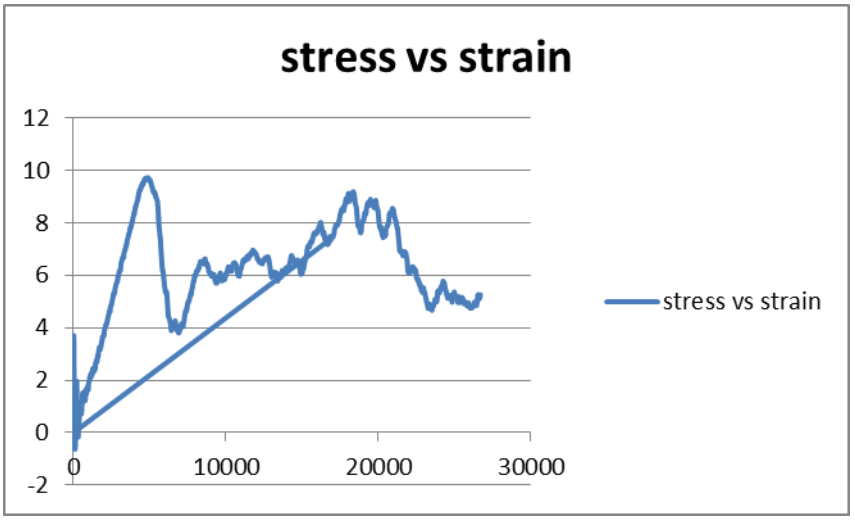

Fig. 4.19: Engineering stress-engineering strain plot for size diameter = 20 Å, height=80 Å (18041 atoms) at strain rate of 3 x 10^9 s^{-1} deformed at 100 K.

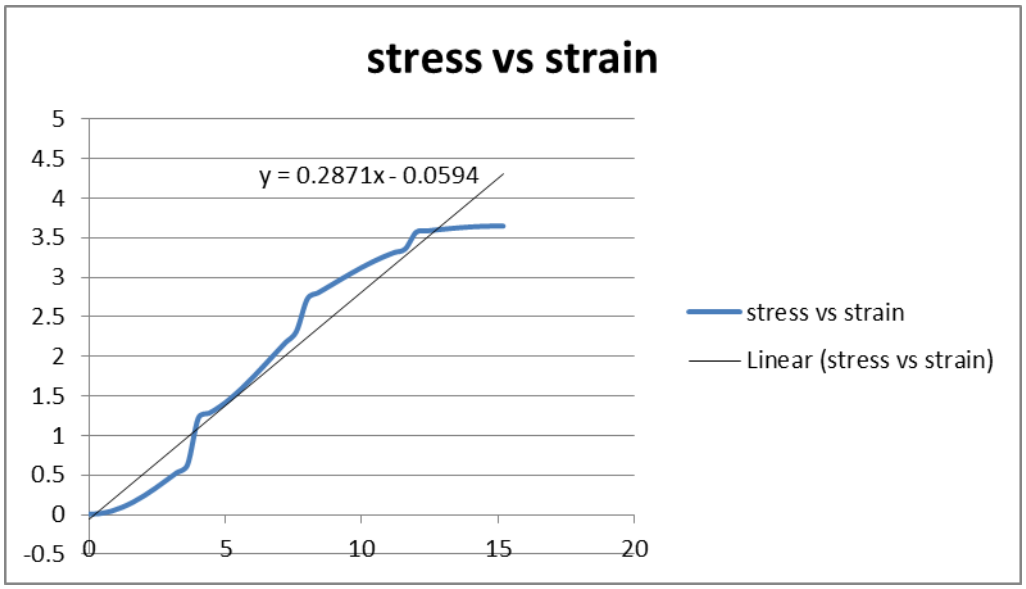

Fig.4.20: A part of graph 4.19 to find Elastic Modulus and first Yield Stress.

From the above graphs, we found different mechanical properties:

Mechanical Prop.	Value (GPa)
UTS (GPa)	9.727475
Rupture Stress (GPa)	5.2564
First Yield Stress (GPa)	3.646247
Elastic Modulus (GPa)	0.2871

Table 4.8: Stress-strain data for size diameter = 20 Å, height =80 Å (18041 atoms) at strain rate of 3 x $10^9 s^{-1}$ deformed at 300 K temperature:

Stress (GPa)	Strain
0.007074	0.00
5.417409	0.05
4.93419	0.01
6.366515	0.15
7.452288	0.20
7.980962	0.25
7.761539	0.30
6.024906	0.35
5.592166	0.40

Based on the data given in Table 4.8, the stress-strain plot obtained has been shown below:

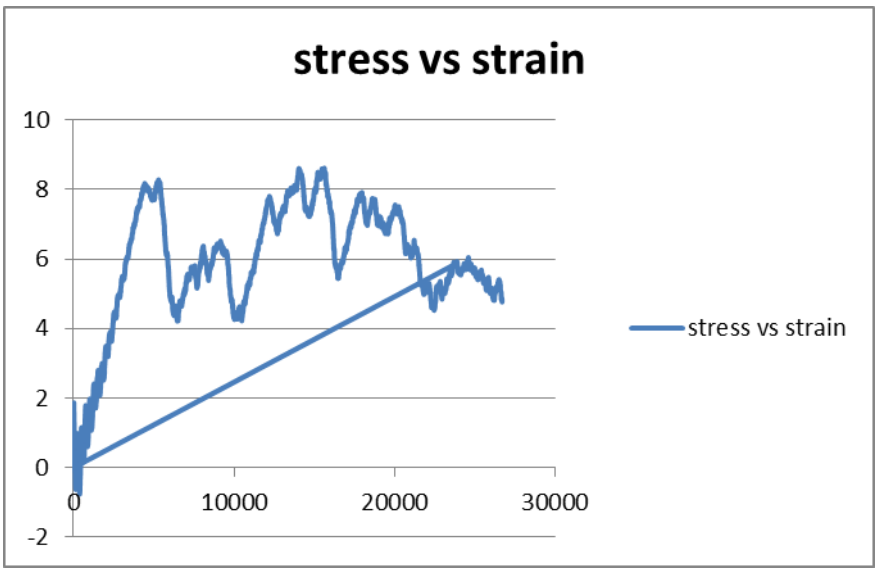

Fig. 4.21: Engineering stress-engineering strain plot for size diameter = 20 Å, height=80 Å (18041 atoms) at strain rate of 3 x 10^9 s^{-1} deformed at 300 K.

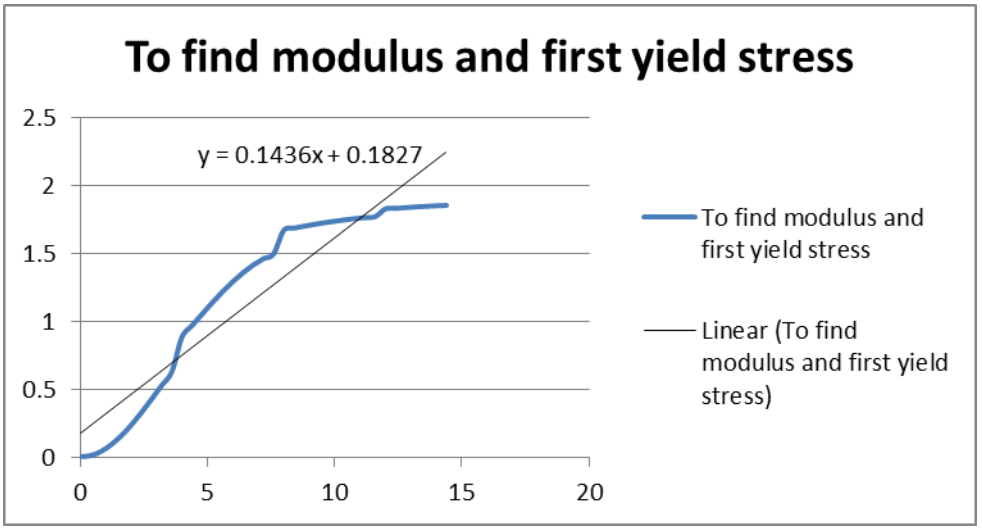

Fig.4.22: A part of graph 4.21 to find Elastic Modulus and first Yield Stress.

From the above graphs, we found different mechanical properties:

Mechanical Prop.	Value (GPa)
UTS (GPa)	8.615013
Rupture Stress (GPa)	4.7621
First Yield Stress (GPa)	1.8555121
Elastic Modulus (GPa)	0.1436

Table 4.9: Stress-strain data for size diameter = 20 Å, height =80 Å (18041 atoms) at strain rate of $3 \times 10^{9} s^{-1}$ deformed at 500 K temperature:

Stress (GPa)	Strain
0.007074	0.00
4.41456	0.05
7.68242	0.01
5.157826	0.15
4.002274	0.20
4.660286	0.25
3.359265	0.30
4.716789	0.35
4.527952	0.40

Based on the data given in Table 4.8, the stress-strain plot obtained has been shown below:

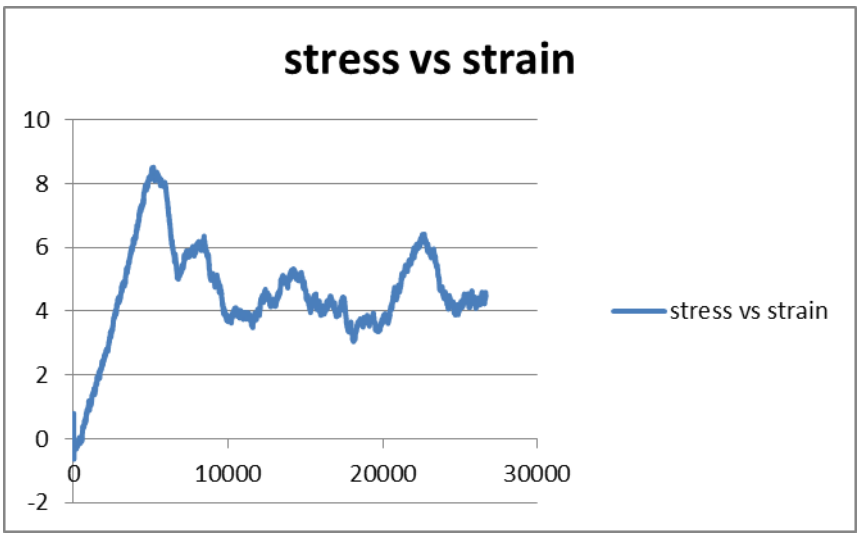

Fig. 4.23: Engineering stress-engineering strain plot for size diameter = 20 Å, height=80 Å (18041 atoms) at strain rate of $3 \times 10^{9}\ s^{-1}$ deformed at 500 K.

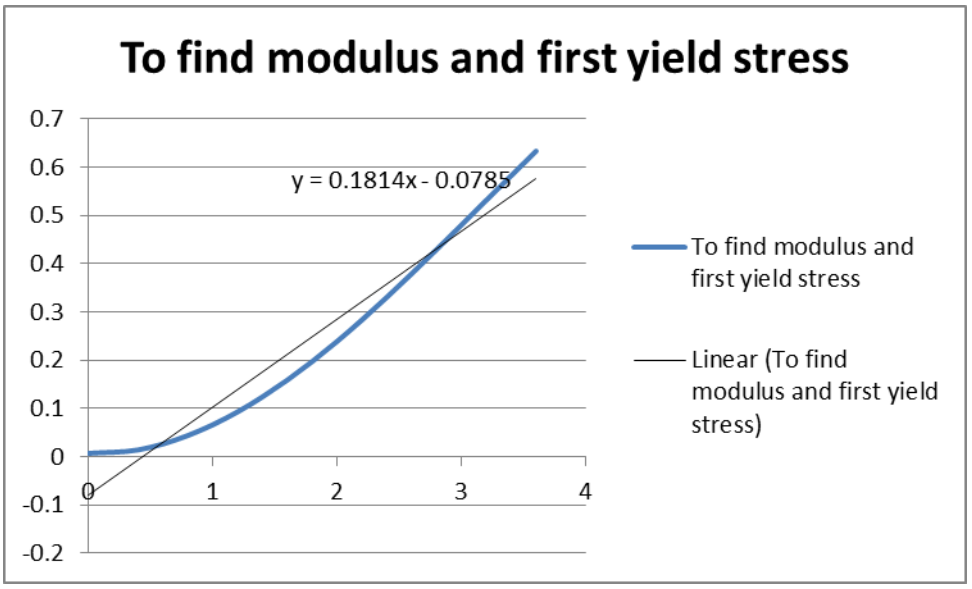

Fig.4.24: A part of graph 4.23 to find Elastic Modulus and first Yield Stress.

From the above graphs, we found different mechanical properties:

Mechanical Prop.	Value (GPa)
UTS (GPa)	8.519249
Rupture Stress (GPa)	4.4971
First Yield Stress (GPa)	0.633043
Elastic Modulus (GPa)	0.1814

Comparison of the stress-strain plots for deformation at different temperatures particular strain rate 3 x 10^9 and size (20 x 80):

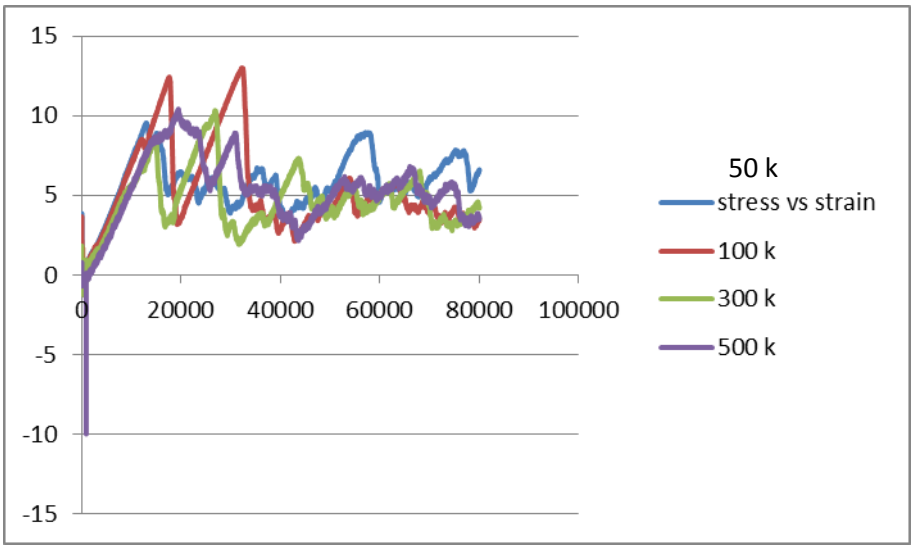

Fig 4.25

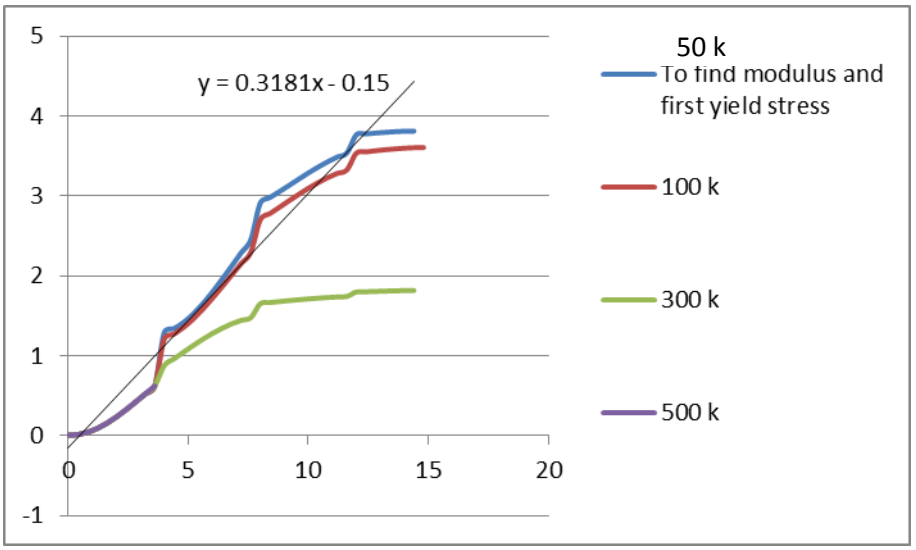

Fig 4.26

- From the above figures & tables we conclude that at particular strain rate as temperature increases the UTS, rupture stress, first yield stress & elastic modulus decrease.
- The maximum Yielding stress decreases as the temperature of ensemble increases. With the increase of ensemble temperature, the thermal oscillations due to numerical corrections & temperature scaling also become dominant [13]

Conclusions:

Form the MD simulations studies on the effect of temperature and strain rate on the deformation behavior of Nickel Nanowires we conclude that:

1. At constant strain rate as temperature range increases from 50 k to 500 k the first yield stress and tensile stress decreases.
2. At constant temperature as strain rate increases from 1×10^{9} s^{-1} to 3×10^{11} s^{-1} the first yield stress and tensile stress increases.
3. At constant strain rate with increase in temperature from 50 k to 500 k the rupture stress and elastic modulus decreases.
4. At constant temperature with increase in strain rate from 1×10^{9} s^{-1} to 3×10^{11} s^{-1} the rupture stress increases, but elastic modulus decreases.
5. The deformation behavior of nanowires with different size at same strain rate and particular temperature is almost similar.

FUTURE WORK:

1. Shape effect on the deformation behavior of Nickel nanowires.
2. Study of atomic paths during deformation.
3. Studying effect of defects on the deformation behavior.

References:

[1]www.wikipedia.com

[2] M.A. Meyers, A. Mishra, D.J. Benson, (2005), Mechanical properties of nanocrystalline materials,pp.479-511

[3] www.lammps.sandia.gov

[4] Satyanarayan Dhal, Yadlapalli Raja, (2012), Effect of temperature and strain rate on deformation behaviour of nickel nanowires: A molecular dynamics simulation study, pp. 20-33, 44-50.

[5] T. Dummer, J. C. Lasalvia, G. Ravichandran and M. A. Meyers, (1998), Effect of strain rate on plastic flow and failure in polycrystallin tungsten, pp.1

[6] Hideyuki Ikeda, Yue Qi, Tahir Çagin, Konrad Samwer, William L. Johnson and William A. Goddard III, (1999), Molecular Dynamics Simulation on Plastic Deformation of Metallic Nanowires, pp. 2-4

[7] Paulo S. Braniicio and Jose-Pedro Rino, (2000), Large deformation and amorphization of Ni nanowires under uniaxia strain: A molecular dynamics study, pp. 1

[8] R. Komanduri, N. Chandrasekaran, L.M. Raff, (2001), Molecular dynamics (MD) simulation of uniaxial tension of some single-crystal cubic metals at nanolevel, pp. 1

[9] W Liang and M Zhou, (2004), Response of copper nanowires in dynamic tensile deformation, pp.1

[10] Yu-Hua Wen, Zi-Zhong Zhua, Gui-Fang Shao, Ru-Zeng Zhu, (2004), The uniaxial tensile deformation of Ni nanowire atomic-scale compute simulations, pp. 1

[11] S. J. A. Koh, H. P. Lee, C. Lu, and Q. H. Cheng, (2004) , The uniaxial tensile deformation of Ni nanowire atomic-scale compute simulations pp. 115

[12] S J A Koh and H P Lee, (2006), Molecular dynamics simulation of size and strain rate dependent mechanica response of FCC metallic nanowires, pp. 5, 9, 15.

[13] Ram Mohan and Yu Liang, (2006), Tensile and Flexural Deformation of Nickel Nanowires via Molecular Dynamics Simulations, pp. 8, 10

[14] www.che.utah.edu/gdsmith/tutorials/tutorial1.ppt